Atmospheric GCM Response to Extratropical SST Anomalies: Synthesis and Evaluation*

Y. KUSHNIR,[+] W. A. ROBINSON,[#] I. BLADÉ,[@] N. M. J. HALL,[&] S. PENG,[**] AND R. SUTTON[++]

[+]*Lamont-Doherty Earth Observatory, Columbia University, Palisades, New York*
[#]*Department of Atmospheric Sciences, University of Illinois at Urbana–Champaign, Urbana, Illinois*
[@]*Laboratori d'Enginyeria Maritima, Universitat Politécnia de Catalunya, Barcelona, Spain*
[&]*Laboratoire des Ecoulements Geophysique et Industriels, Grenoble, France*
[**]*NOAA–CIRES Climate Diagnostics Center, University of Colorado, Boulder, Colorado*
[++]*Centre for Global Atmospheric Modeling, Department of Meteorology, University of Reading, Reading, Berkshire, United Kingdom*

(Manuscript received 24 August 2001, in final form 23 January 2002)

ABSTRACT

The advances in our understanding of extratropical atmosphere–ocean interaction over the past decade and a half are examined, focusing on the atmospheric response to sea surface temperature anomalies. The main goal of the paper is to assess what was learned from general circulation model (GCM) experiments over the recent two decades or so. Observational evidence regarding the nature of the interaction and dynamical theory of atmospheric anomalies forced by surface thermal anomalies is reviewed. Three types of GCM experiments used to address this problem are then examined: models with fixed climatological conditions and idealized, stationary SST anomalies; models with seasonally evolving climatology forced with realistic, time-varying SST anomalies; and models coupled to an interactive ocean. From representative recent studies, it is argued that the extratropical atmosphere does respond to changes in underlying SST although the response is small compared to internal (unforced) variability. Two types of interactions govern the response. One is an eddy-mediated process, in which a baroclinic response to thermal forcing induces and combines with changes in the position or strength of the storm tracks. This process can lead to an equivalent barotropic response that feeds back positively on the ocean mixed layer temperature. The other is a linear, thermodynamic interaction in which an equivalent-barotropic low-frequency atmospheric anomaly forces a change in SST and then experiences reduced surface thermal damping due to the SST adjustment. Both processes contribute to an increase in variance and persistence of low-frequency atmospheric anomalies and, in fact, may act together in the natural system.

1. Introduction

a. The problem

The interaction between the ocean and the atmosphere is a key to understanding and predicting climate variability. This review addresses one aspect of this problem, the interaction between the extratropical ocean and its overlying atmosphere. Early research on this problem includes the pioneering work of Namias (Namias 1959, 1965a,b, 1972), who sought to establish methods for short-term climate prediction, and that of Bjerknes (Bjerknes 1959, 1964), who set the stage for the present-day study of decadal climate variability. Recent advances in understanding tropical atmosphere–ocean interactions, specifically the El Niño–Southern Oscillation (ENSO) phenomenon, and the success in applying this understanding to climate prediction, spurred interest in the extratropical interaction as the next challenge in developing a more skillful climate prediction system. Moreover, the search for the causes of decadal climate variability and for perplexing shifts and trends in key circulation indices, including that of ENSO, have fueled the debate over the role of the extratropical oceans in long-term climate variability (Latif and Barnett 1994, 1996; Gu and Philander 1997; Saravanan et al. 2000; Marshall et al. 2001).

Here we take the view that the ocean participates in climate variability through anomalies in the sea surface temperature, and we address the question of how the atmosphere responds to such anomalies. Extratropical SST anomalies are generated mainly by the atmosphere, through turbulent fluxes of moist static energy at the air–sea interface, or through wind stress anomalies that cause turbulence and shallow (Ekman) currents in the upper ocean (e.g., Junge and Haine 2001). As described in the comprehensive review by Frankignoul (Frankignoul 1985, hereafter F85) the theoretical basis for understanding the atmospheric influence on the extratrop-

* Lamont-Doherty Earth Observatory Contribution Number 6329.

Corresponding author address: Dr. Yochanan Kushnir, Lamont-Doherty Earth Observatory, Columbia University, Palisades, NY 10964.
E-mail: kushnir@ldeo.columbia.edu

ical ocean was established in the 1960s and 1970s (e.g., Kraus and Turner 1967; Gill and Niiler 1973; Niiler and Kraus 1977; see also F85) and convincing observational support for this theory has continued to accumulate since (see section 2 below). Over most of the extratropical ocean, SST variability emerges primarily as a local response to fluctuations in the surface atmospheric conditions, such as wind speed, temperature, and humidity that cause changes in air–sea heat fluxes (Frankignoul and Hasselmann 1977; Frankignoul and Reynolds 1983; F85). This does not mean that the extratropical interaction is one-way. On the contrary, while changes in air–sea fluxes modify the SST they also affect the temperature and humidity of the marine boundary layer. The adjustment of both ocean and atmosphere results in smaller surface energy fluxes than would otherwise occur (Barsugli and Battisti 1998; Frankignoul et al. 1998; see also section 5a below). If this local thermodynamic coupling were all that it entailed, the extratropical interaction would stand in sharp contrast to the *dynamically coupled* tropical interaction associated with ENSO. In the latter, SST anomalies are determined by changes in ocean heat transport resulting from a nonlocal, delayed interaction with the atmosphere, and they are damped by surface energy fluxes (e.g., Neelin et al. 1998). In the tropical Pacific, the atmosphere responds to a SST anomaly through a local, thermally direct change in the circulation, involving a deep convection anomaly, and a shift in the midtropospheric centers of latent heat release. Consistent with this are changes in large-scale surface convergence and upper-tropospheric divergence patterns, affecting the entire tropical belt. Such changes in the tropical circulation also have a marked effect outside the tropical troposphere, as described in numerous publications (see reviews by Neelin et al. 1998; Trenberth et al. 1998). Such effects, however, are not expected to occur in the extratropical atmosphere, because the amounts of latent heat released through extratropical convection are much smaller than in the Tropics and are confined to a shallower layer of the lower troposphere. Yet, because of the generally deep mixed layers associated with extratropical SST anomalies (during winter), changes in the latter represent large anomalies in upper-ocean heat content. Such changes are persistent (see section 2 for further discussion) and could potentially enhance the persistence of extratropical atmospheric anomalies and render them more predictable. *Thus the question central to this review, and to the debate on the role of the ocean in extratropical climate variability, is whether the influence of the extratropical ocean extends beyond the local thermodynamic response of the marine boundary layer to affect the evolution and dynamical properties of the large-scale atmospheric circulation.*

In an effort to identify the overall effect of the extratropical ocean on the atmosphere, general circulation model (GCM) experiments have been conducted, in which the climatological SST distribution is perturbed and the response to that perturbation examined (F85). These experiments have been justified by the difficult task of untangling the oceans' ''back interaction'' on the atmosphere from observations. The notion has always been that modeling the behavior of the individual components of the coupled system will lead to a better understanding of the whole. While this approach can be misleading (see the discussion in section 5), it has been extremely successful when applied to understanding the local and remote effects of ENSO (Trenberth et al. 1998), and it serves as the basis for several current climate prediction schemes (e.g., Barnett et al. 1994). Attempts to apply GCMs to the extratropical problem, however, seem to have failed to provide the consistent and incontrovertible results found in the tropical setting (F85). Thus, progress in addressing the extratropical problem has been frustratingly slow.

Despite the difficulties in interpreting extratropical SST experiments and in reconciling the differences among them, most of them tend to agree broadly regarding the strength of the response and the processes important for its maintenance (reviewed in section 4 below). Moreover, the recent application of coupled models (see section 5) has provided new ideas regarding the nature of the midlatitude atmosphere–ocean interaction and its role in climate variability. We feel, therefore, that a summary of the current understanding is timely.

b. Goals and format of this paper

This paper is a critical review of the progress in understanding the dynamical atmospheric response to extratropical SST anomalies, emerging from recent observational and theoretical analysis and particularly from recent atmospheric GCM experiments. Our goal is to point out the areas of agreement and disagreement among representative studies and to evaluate the degree to which the inconsistencies are or can be resolved. We seek to contribute to the debate over the role of surface anomalies in climate variability and climate change by drawing conclusions regarding the nature of the extratropical interaction and the climatic influence of midlatitude SST variability. In addition, we hope to provide insights that will aid in the use of coupled models in climate prediction.

The paper begins where the F85 review left off, and it ends with the most recent published work. Some review of prior material is added where it is needed for completeness. We start with a survey of the observations in section 2 and of the theory regarding the response of the atmosphere to SST anomalies in section 3. These sections are intended as background for the discussion of GCM modeling results that follows. Our discussion of recent GCM experiments in section 4 begins by examining the response in experiments forced with fixed (often simplified) SST anomalies and continues with a review of GCM experiments forced with realistic, time-

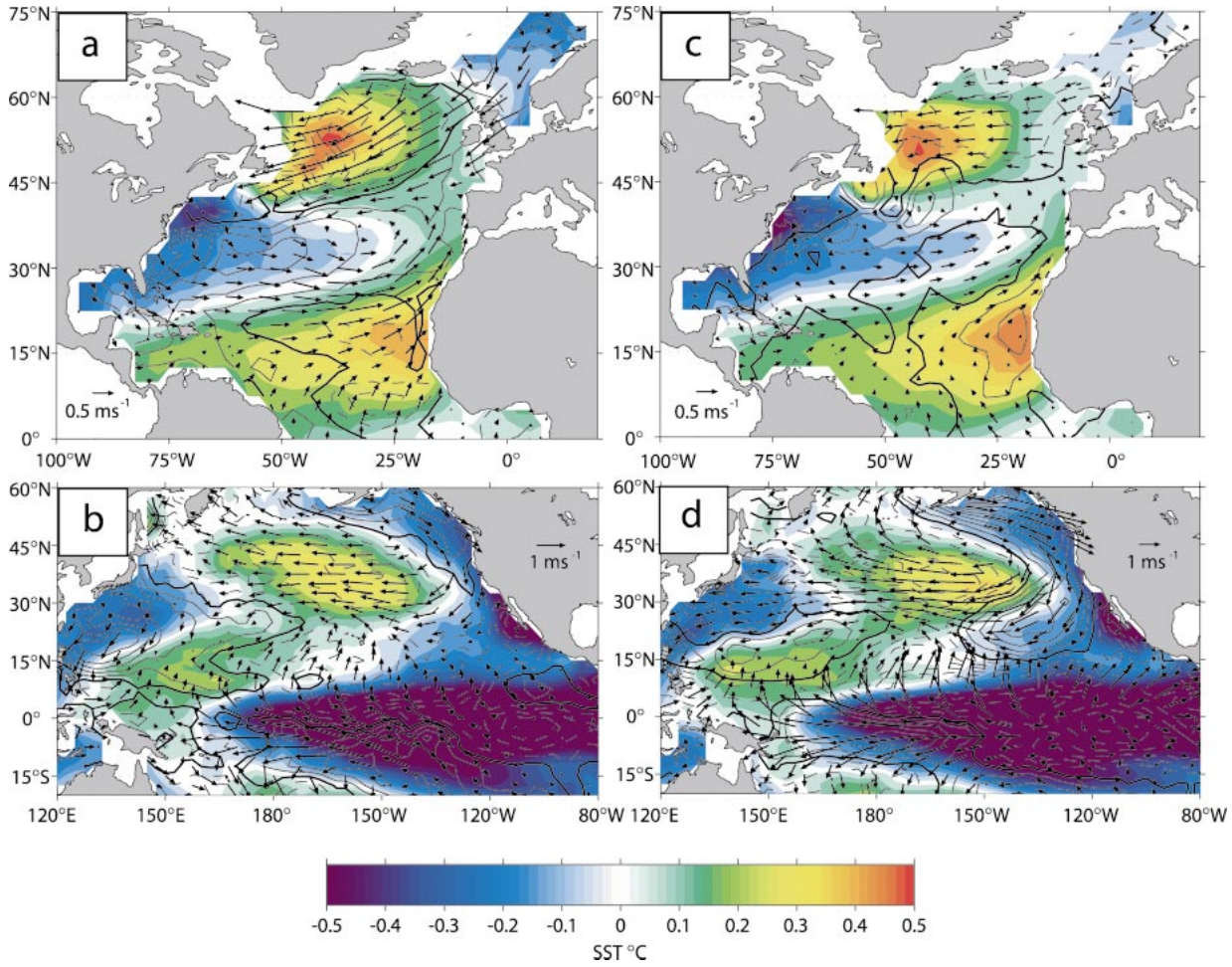

FIG. 1. The patterns of wintertime (Dec–Mar), anomalous SST, ocean–atmosphere turbulent heat flux (latent plus sensible), and surface wind vectors, associated (via linear regression) with the leading PC of SST variability in the (a), (c) North Atlantic and (b), (d) North Pacific. (a), (b) The observations from 1949 to 1999 (data from NCEP–NCAR reanalysis). (c), (d) The mean of a 10-member ensemble GCM integrations forced with global, time-varying SST anomalies from 1950 to 1999 (ECHAM3.5 GCM data provided by L. Goddard). Heat fluxes are in W m^{-2} with positive (negative) values in solid (dashed) contours every 3 W m^{-2}. The zero contour is bold. Arrows depict the wind vectors in m s^{-1} with scales as shown in panels. The SST anomaly values (C°) are denoted in colors according to scale (note that scale is kept at the −0.5°–0.5°C range for overall clarity, however, values in eastern equatorial Pacific extend up to 1.2°C).

varying SST anomalies [AMIP (Atmospheric Model Intercomparison Project) type experiments]. Finally, in section 5, we discuss the recent extension of the investigation to the realm of coupled model experiments. Conclusions follow in section 6.

2. The observed pattern of extratropical atmosphere–ocean anomalies

a. Fundamental properties of extratropical SST anomalies

As described in F85, The salient features of observed extratropical SST anomalies and their associated atmospheric patterns are as follows:

- Extratropical SST anomalies have large, basin-size, scales. While small-scale perturbations in SST (associated with mesoscale ocean eddies) are visible in high-resolution data, there is a distinct large-scale signature in midlatitude SST variability that is similar to the scale of atmospheric low-frequency variability (Namias and Cayan 1981; Wallace and Jiang 1987; and Figs. 1a,b).
- SST anomalies are the surface expression of changes in the heat content of a well-mixed upper-ocean layer that represents a large thermal reservoir. This property grants SST anomalies large persistence compared to atmospheric anomalies. The *e*-folding timescale of midlatitude SST anomalies is typically 3–5 months (Barnett 1981; Frankignoul and Reynolds 1983).
- Over most of the World Ocean, monthly and seasonal extratropical SST anomalies are well correlated with the overlying surface air temperature anomalies (F85, see section 2.3).

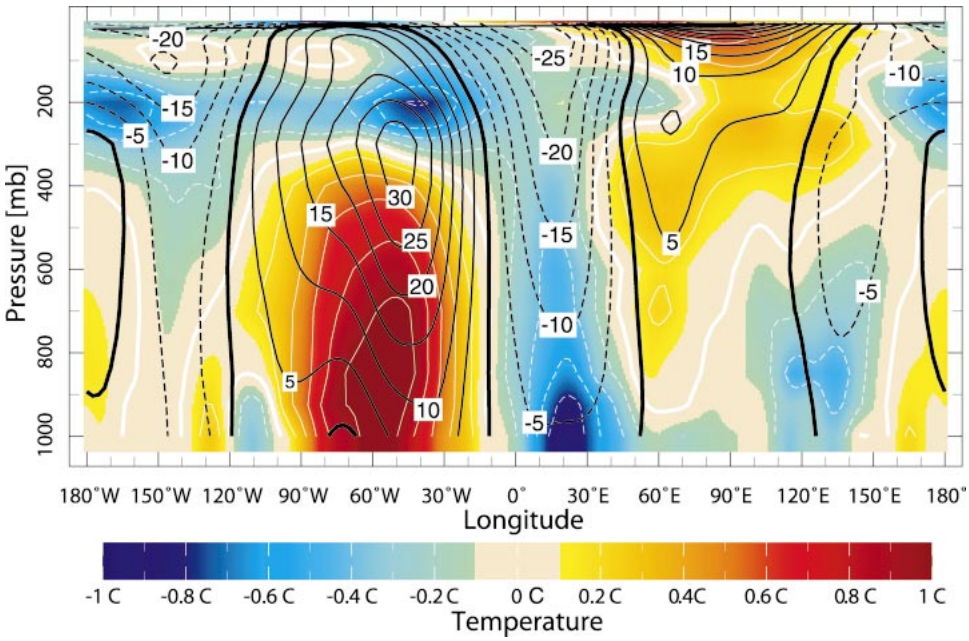

FIG. 2. A vertical cross section along the latitude of 52.5°N of the wintertime (Dec–Mar) air temperature and geopotential height anomalies associated (via linear regression) with the leading PC of North Atlantic SST (shown in Fig. 1a). Air temperature anomalies are shown in colors and white contours every 0.2°C, with positive (negative) areas in shades of red (blue) (see scale at bottom) and solid (dashed) contours for positive (negative) values. Geopotential height anomalies are in black contours every 5 m with positive (negative) values in solid (dashed) contours. The analysis is based on NCEP–NCAR reanalysis data.

- In the extratropics, the dominant patterns of monthly and seasonal SST anomalies are well correlated with the primary patterns of atmospheric circulation anomalies. This association is strongest during winter and is largest when the atmosphere leads the ocean by about a month (Davis 1976, 1978; Wallace and Jiang 1987).
- As shown in Figs. 1a,b, negative extratropical SST anomalies are associated with stronger than normal surface westerlies above (and straddled by a pair of sea level pressure anomalies, a cyclone poleward, and an anticyclone equatorward). The opposite is true for positive SST anomalies.
- During winter, the atmospheric anomalies associated with SST variability display an equivalent barotropic vertical structure, that is, the typical signature of internal atmospheric low-frequency variability (Fig. 2).

These observations convinced pioneers of climate research (e.g., Namias 1959, 1965a,b; Bjerknes 1964) and those who followed (e.g., Davis 1976, 1978; Barnett 1981; Weare 1977) that extratropical SST anomalies are forced by surface flux and Ekman current anomalies arising from changes in surface wind speed, surface air temperature, and surface humidity. At the same time, a hypothesis emerged that extratropical SST anomalies imprint their large persistence on atmospheric variability and could thus be used for short-range climate prediction (e.g., Namias 1969, 1972; Namias and Cayan 1981; Ratcliffe and Murray 1970; Barnett and Somerville 1983). However, determining the nature and strength of the oceans' back interaction on the atmosphere has remained a challenge, and has been the main reason for the use of GCMs in controlled experiments with prescribed SST forcing.

b. Recent studies of ocean–atmosphere data and their implications

1) SURFACE FLUX FORCING OF SST ANOMALIES

Cayan (1992a,b,c) conducted a systematic observational study of the relationships among atmospheric sea level pressure anomalies, air–sea fluxes (sensible and latent), and SST variability. Figures 1a,b, inspired by similar figures in Cayan's papers, show a key relationship between the prominent seasonal anomalies in the Northern Hemisphere surface circulation and the underlying surface flux and SST anomalies. Coherent flux anomalies, with spatial scales comparable to those of anomalies in the atmospheric low-frequency circulation, appear at the sea surface and correspond to the SST anomaly patterns. The anomalous surface heat flux is from the ocean to the atmosphere in areas where SST is colder than normal and vice versa (i.e., the correlation between the upward surface flux and SST is negative). Cayan showed that the anomalies in surface heat flux are explained by large-scale anomalies in wind speed, surface air humidity, and air–sea temperature difference,

and that the surface heat flux variability determines the large-scale SST tendency.

Cayan's (1992a,b,c) studies and a more recent surface heat budget analysis by Seager et al. (2000) showed that local changes in wind speed and in the horizontal advection of heat and moisture in the marine boundary layer can be equally important in determining extratropical surface flux variability and, hence, monthly and seasonal SST variability. Anomalous advection within the atmospheric boundary layer can force anomalies in air temperature and humidity; inducing a response in the surface heat flux that maintains the balance of enthalpy in the marine boundary layer. This is particularly true near continental boundaries in winter, where changes in wind speed and direction affect the amount of cold, dry air reaching the ocean. In the absence of strong advection, the boundary layer temperature and humidity partially adjust to the wind speed–forced SST anomaly (Seager et al. 1995; see also section 5). In addition to these thermodynamic effects, wind stress fluctuations also produce anomalous Ekman currents, which act on the mean temperature gradient in the ocean to create SST anomalies (Namias 1965; Frankignoul 1985; Luksch and von Storch 1992; Seager et al. 2000). The anomalous Ekman current contributions to SST anomalies in both the North Atlantic and North Pacific Oceans are generally in phase with the local surface flux forcing and, in some locations, are of the same order of magnitude (Seager et al. 2000).

The degree of symmetry in the time-lagged cross correlation between SST anomalies and the associated atmospheric patterns has been used to assess the causal link between the two and to indicate possible feedback from the ocean to the atmosphere. Results that show atmospheric geopotential height variability leading that of SST by a month or so, indicating that the former drives the latter, date back to the mid-1970s (Davis 1976, 1978). An analysis of weekly SST and 500-hPa height data by Deser and Timlin (1997) puts the atmospheric lead at 2–3 weeks. Frankignoul et al. (1998) calculated the cross correlation between surface flux and SST. They found that in the mid–North Atlantic, when the atmosphere–ocean flux leads SST, the local correlation between the two variables is positive, indicating that the SST is forced by the flux. The correlation changes sign at zero lag and becomes negative, implying that when the atmospheric perturbation that drive SST anomalies disappear or weaken, the anomalies decay by losing heat to the atmosphere. The rate of SST decay is about 20 W m^{-2} K^{-1}, corresponding to a decay time of about 120 days for a thermal anomaly in a 50-m-deep oceanic mixed layer.

2) FALL SEASON REEMERGENCE OF WINTER-FORCED SST ANOMALIES

Namias and Born (1970), Wallace and Jiang (1987), and Namias et al. (1988), noted a significant correlation between North Pacific SST anomalies in the spring and in the following fall. They hypothesized that SST anomalies formed by atmospheric surface fluxes during winter are hidden beneath a shallow, stable layer during summer, only to reemerge in the fall, when stirring by the wind and surface heat fluxes erode the sheltering layer. Alexander et al. (1999) presented time–depth cross sections of ocean temperature correlations in several North Pacific locations. These results show that winter and spring SSTs are significantly correlated with summer temperature only in the deeper part of the upper ocean (below the seasonal mixed layer) but not at the surface. In the ensuing fall however, large correlations to previous winter SST reappear at the surface (and throughout the entire mixed layer). Thus, it is plausible that the fall atmosphere experiences the impact of ''ocean-imposed'' SST anomalies that are not forced by concomitant surface flux variability.

3) EVIDENCE FOR AN ATMOSPHERIC RESPONSE

Recently, Czaja and Frankignoul (1999, 2002) presented observational evidence consistent with an atmospheric response to reemerging SST anomalies. They examined the correspondence between SST and 500-hPa anomalies at different lags over the entire year, in contrast with earlier work that concentrated on the winter season. In so doing, Czaja and Frankignoul found a statistically significant covariance between the 500-hPa heights during winter and the SST up to six months earlier (SST from the previous fall, summer, and spring). Rodwell and Folland (2002, manuscript submitted to *Quart. J. Roy. Meteor. Soc.*, hereafter RF02) present similar results. In both analyses, the atmospheric ''response'' displays the pattern of the North Atlantic Oscillation (NAO)—the most prominent prototype of atmospheric variability in the Atlantic basin, featuring anticorrelated fluctuations in the strengths of the Icelandic low and the Azores high.

Care must no doubt be taken when assigning cause and effect on the basis of correlations between two variables, lest the relationship is caused by a third, external variable, such as remote forcing from outside the North Atlantic basin. However, the link between ocean and atmosphere at such long leads, in the studies described above, seems to stem from the remarkable persistence of the North Atlantic SST anomalies throughout the year—a persistence that can be explained by the thermal inertia of the oceanic mixed layer and by reemergence. Figure 3a displays evidence for this persistence. The autocorrelation of the first principal component (PC) of year-round North Atlantic SST anomalies is plotted as a function of the calendar month (shown along the ordinate). In winter, the PC times series is associated with the SST pattern depicted in Fig. 1a. Along a horizontal line starting at an arbitrary calendar month (from September to September, centered on March) are plotted the correlations between that month's PC value and its values in each calendar month beginning March of the

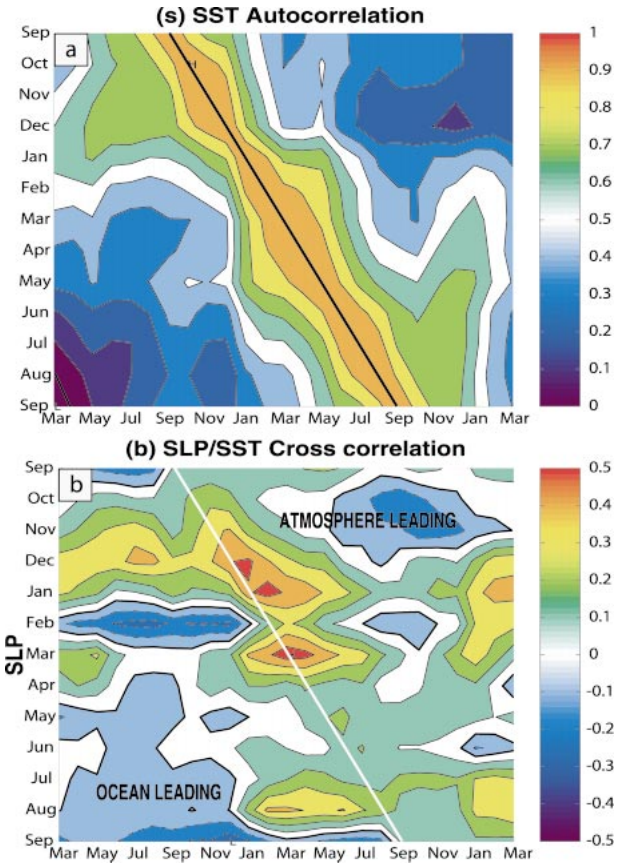

FIG. 3. (a) The autocorrelation function of the first PC of monthly, year-round North Atlantic SST anomalies, plotted as a function of the calendar month. Contours and colors show the correlation between the PC values in the month shown on the ordinate and that shown on the abscissa, with the instantaneous correlations (value of 1.0) indicated by the thick, solid black line along the diagonal. (b) Cross correlation between the first PC of monthly, year-round SLP, and the first PC of monthly, year-round North Atlantic SST anomalies. Contours and colors show the correlation between the SLP PC values in the month shown on the ordinate and SST in the month shown on the abscissa, with instantaneous cross correlations indicated by the thick solid white line along the diagonal. The analysis is based on NCEP–NCAR reanalysis data, 1958–98.

previous year and ending with March of the following year (as indicated on the abscissa). The simultaneous correlations (value of 1.0) appear along the diagonal and are indicated by a thick black line. The leading pattern of SST variability in the North Atlantic is remarkably persistent (the 95% level in this diagram is ~0.5) from spring (March–May) into the ensuing fall and early winter (November–January).

Figure 3b shows the cross correlation between the first PC of SST and the leading atmospheric pattern derived from a similar, year-round analysis of monthly mean sea level pressure (SLP) anomalies in the Atlantic sector. This pattern strongly resembles the NAO and is, during winter, consistent with the wind pattern depicted in Fig. 1a. The cross-correlation function is presented in a manner analogous with Fig. 3a. SLP correlations with SST values from March of the previous year to March of the following year are plotted, month by month, along lines parallel to the abscissa for the entire year, beginning in September. Instantaneous correlations are indicated by the thick white diagonal line. The 95% confidence level for this diagram is ~0.25 (tested using a bootstrap procedure). Consistent with the results of Czaja and Frankignoul (1999, 2002) and of RF02, SLP values during the fall to winter transition are significantly, albeit weakly, correlated with SST in the previous spring and summer (note the yellow-colored region in Fig. 3b). During winter, SLP–SST correlations are highest when SLP leads SST by one month, as described in section 2a.

4) DECADAL VARIABILITY

Not all of extratropical SST variability should be ascribed to local heat exchange with the atmosphere. Bjerknes (1964) noticed that the relationship between North Atlantic SST and the atmosphere is timescale dependent. He found that multiyear SST anomalies persist in the Gulf Stream extension region, south of the Grand Banks, which are quite different from the pattern of interannual SST variability (see Bjerknes 1964, their Fig. 21). Bjerknes argued that the decadal SST anomalies are caused by a change in the strength or position of the wind-driven, subtropical gyre, in response to multiyear changes in the basin-scale atmospheric circulation. This interesting idea lay dormant until the 1990s, when interest in anthropogenic climate change drew attention to decadal climate variability. Timescale dependence and decadal variability in SST were recently found in the North Atlantic (Deser and Blackmon 1993; Kushnir 1994) and the Pacific (Zhang et al. 1997; Nakamura et al. 1997), confirming and extending the ideas proposed by Bjerknes. The possibility that the extratropical SST varies through changes in oceanic heat advection, reminiscent of phenomena associated with El Niño, was suggested by numerical simulations with ocean models (see Seager et al. 2001; and references therein) and spurred speculations regarding a new, predictable form of extratropical atmosphere–ocean interaction (e.g., Latif and Barnett 1994). Such interaction is possible however, only if the atmosphere responds to the SST anomalies.

5) TROPICAL VERSUS MIDLATITUDE FORCING

The possible link between tropical and extratropical SST anomalies was not fully addressed in early diagnostic work. This issue is important, because tropical SST anomalies, particularly in the Pacific, are predictable and generate global atmospheric teleconnections. The subject of tropically driven variability in the atmosphere and its influence on extratropical SST is dealt with in a companion paper (Alexander et al. 2002, this issue). SST anomalies related to tropical forcing introduce additional uncertainty in interpreting atmosphere–

ocean interactions in observations and models, and their influence should not be neglected.

3. Theoretical background: Atmospheric response to fixed SST anomalies

a. General remarks

In considering the atmospheric response to oceanic forcing, we break into a coupled system, and treat interactions in one direction only. The theory discussed in this section describes how an oceanic thermal anomaly can deliver to the atmosphere information stored by the ocean's thermal capacity or transmitted by ocean currents. This theory is only part, albeit an essential one, of an understanding of the fully coupled system. Even the one-way interaction problem, however, must be idealized if it is to be tractable. A large class of theoretical models is based on a linearized version of the geostrophic or primitive system of equations. A choice must be made to consider the atmospheric response to either an imposed SST anomaly or an imposed corresponding atmospheric heating anomaly. The former approach is taken in full GCM experiments, because these models calculate the surface heat flux and the subsequent sensible and latent heating within the atmosphere as the latter responds to the SST change, but theoretical models, linear or nonlinear, commonly use prescribed heating anomalies to represent the SST effect. Theoretical studies usually examine the stationary response to the SST-related perturbation, while GCM integrations are time dependent. This section examines the hierarchy of theoretical models used to study the extratropical response to surface heating anomalies.

b. Linear response to heating

The magnitude of a dynamical atmospheric response in midlatitudes is often measured as the 500-hPa height response to a surface thermal anomaly. An estimate of the largest perturbation likely to arise from a midlatitude SST anomaly can be established by vertically integrating the hydrostatic equation. Imagine that the entire lower half of the troposphere has come into thermal equilibrium with an SST anomaly, T_0', though this is surely an overestimate of the possible effects of the surface flux on the local change of air temperature. Thus, a temperature perturbation exists between $p = (1000 + p'_{\text{surface}})$ hPa and $p = 500$ hPa, and the hypsometric equation gives

$$z'_{500} \approx \overline{z}_{500}\left(\frac{T'_o}{\overline{T}_a} + \frac{1}{\ln 2}\frac{p'_{\text{surface}}}{1000}\right). \tag{3.1}$$

For $T_0' = 1$ K, the baroclinic contribution to z' from the first term is about 20 m. The barotropic contribution, if it exists, will add or subtract about 7 m for every 1 hPa of surface pressure perturbation, p'_{surface}, and should not be overlooked. The direct linear, geopotential height response to atmospheric heating, discussed below, invariably features a surface low beneath the upper-air high, thereby weakening the hydrostatic, upper-air response. When midlatitude dynamical feedbacks are included, however, the surface pressure response may have the same sign as the geopotential response aloft. The observed standard deviation of 500-hPa heights on monthly to interannual timescales is of the order of 50–100 m. Thus, while it is possible for the response to an SST anomaly to provide a significant signal at the 500-hPa level, this signal is almost certainly smaller than the unforced variability, and might be hard to detect in GCM integrations. To proceed to a more realistic quantitative solution, nonlocal dynamical effects must be included. An excellent discussion of theoretical and modeling studies of the effect of diabatic heating in the midlatitude atmosphere is provided in F85. Only a summary of the principal conclusions is provided here.

In quasigeostrophic theory, relevant to the extratropics, a heating anomaly acts as a source of potential vorticity below the level of maximum heating, where heating tends to increase the static stability, and a sink above the heating, where heating tends to decrease the static stability.[1] Surface heating, if present, is equivalent to a source of potential vorticity at the lower boundary,[2] but there is a compensating sink immediately above the surface, if the heating decreases with height. The vertically integrated potential vorticity source from heating is exactly zero, so heating cannot directly force a barotropic response.

If, as is generally the case, the response is at least partially in phase with the forcing, there is positive potential vorticity with its associated negative geopotential anomaly at low levels, and negative potential vorticity with its associated positive geopotential anomaly aloft. As described in Hoskins and Karoly (1981), at lower-tropospheric levels, the thermodynamic energy equation determines the pattern of the response: the heating is balanced by either zonal or meridional temperature advection, depending on the depth of the heating. For deep heating, meridional advection dominates, requiring a downstream shift in the surface low. For shallow heating, zonal advection is also important, requiring a baroclinic warm core structure, shifted downstream from the heat source (Hoskins and Karoly 1981). At upper levels, the vorticity equation determines the balance, and the potential vorticity sink can be balanced either by zonal advection, implying a low west of the heating and a high downwind, or by meridional advection across the mean potential vorticity gradient, implying a downstream low. For the horizontal spatial scale of a typical SST anomaly, zonal advection dominates, giving a

[1] In the QG framework potential vorticity q, is given by $q = \beta y + \varsigma - \partial/\partial p[(f_0/\sigma)(RT/p)]$. Because heating, Q, drives a temperature change, dT/dt, the rate of change of potential vorticity is related to the vertical gradient of Q, or $dq/dt + \cdots = -\partial/\partial p[(f_0/\sigma)(RQ/p)]$.

[2] In this case, the heating enters as a lower boundary condition on q: $dq_b/dt + \cdots = (f_0/\sigma)(RQ/p_b)$, where $q_b = (f_0/\sigma)(RT/p)|_b$.

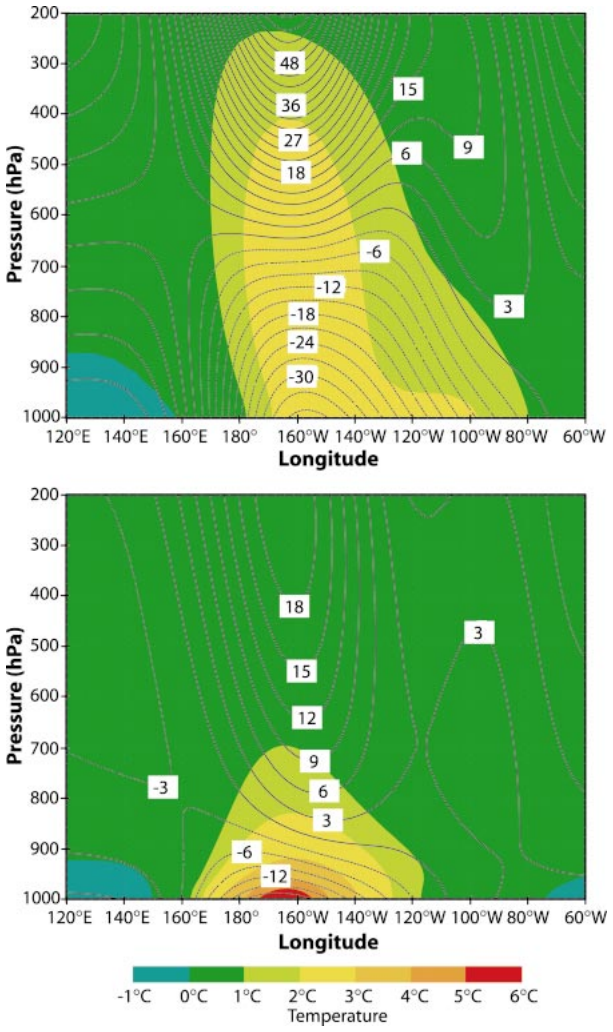

FIG. 4. The response to (top) deep and (bottom) shallow heating of the linear quasigeostrophic model in a wide β channel with a westerly, baroclinic jet in its center. Colors indicate the perturbation temperature (every 1 K, see color scale at bottom) and contours show the geopotential height perturbation (every 3 m). The heating is centered at the date line (180°) and decays exponentially with height.

downstream high (Hoskins and Karoly 1981; Hendon and Hartmann 1982; Held 1983).

Figure 4 shows the typical, linear, quasigeostrophic responses to heating. The results are for a wide β-channel, where the zonal flow is a westerly baroclinic jet, centered in the middle of the channel, far from its sides. In both panels, the heating, centered at the longitude of 180°, is strongest at the surface and decays exponentially with height. Regardless of whether the heating is shallow (left) or deep (right), the response is baroclinic, with a surface low east of the heating.

As realism is added to the linear problem, moving from the quasigeostrophic framework to the primitive equations on a sphere with realistic, spatially varying basic states and complex heat sources, the solutions become correspondingly more complicated in their spatial structure. Such analyses have been carried out for extratropical thermal forcing by Hoskins and Karoly (1981), Hendon and Hartman (1982), Valdes and Hoskins (1989), Ting (1991), Ting and Peng (1995), and Peng and Whitaker (1999). These studies show a common vertical structure in the response, even when the heating is allowed to interact dynamically with the flow field (as is the case with a bulk aerodynamic formula parameterization of surface sensible heat flux). Hall et al. (2001) show several typical examples of the linear response to midlatitude heating in a realistic basic state. Despite the zonally asymmetric basic state, these time-independent solutions display the same surface low and upper-level high downstream, when a positive heating anomaly is imposed, as seen in the quasigeostrophic, zonally symmetric setting. Realistic variations either in the basic state or in the position of the SST anomaly can cause noticeable modifications of the response. In particular, the results display visible sensitivity to the location of the heating with respect to the jet. GCM responses to extratropical SST anomalies, however, display greater sensitivity to the underlying climatology than is evident in the linear calculations of Hall et al. (2001) and some even display an equivalent barotropic response that is reminiscent of the observed SST–atmosphere relationship [see section 4b(1)], suggesting the need to consider nonlinear processes.

c. Nonlinear response to heating

The fact that nonlinearity can be an important factor in the response to a midlatitude SST anomaly has been established in a statistical analysis of many long integrations of a simple atmospheric GCM by Lunkeit and von Detten (1997). In a suite of experiments with varying amplitude and sign of the prescribed SST anomalies, they found statistically significant evidence that the response amplitude is linearly related to the forcing only over a narrow range of anomaly values and that linearity fails if the sign of the anomaly is reversed. They also observed changes in the pattern of the response with the size of the prescribed anomaly. Similarly, in a realistic GCM with a North Atlantic SST anomaly, which was integrated to produce an extensive ensemble of realizations, Peng et al. (2002) found that the atmospheric response depends both on the season and on the sign of the forcing.

To illustrate the difficulties of diagnostically resolving a nonlinear system, consider the linear system formally expressed as

$$\frac{d\boldsymbol{\Psi}}{dt} = \mathbf{L}(\boldsymbol{\Psi}) + \mathbf{f}(t). \tag{3.2}$$

Here $\boldsymbol{\Psi}$ is a linear solution vector that completely characterizes the anomalous flow, $\mathbf{L}$ is a linear operator, and $\mathbf{f}$ is forcing, such as the heating associated with an SST anomaly. The stationary solution is given by

$$\overline{\boldsymbol{\Psi}} = -\mathbf{L}^{-1}\overline{\mathbf{f}}. \quad (3.3)$$

In a similar way, the equilibrium response of a model with quadratic (advective) nonlinearity can be expressed as a solution to the equation:

$$\mathbf{L}(\overline{\boldsymbol{\Psi}}) + \overline{\boldsymbol{\Psi}}^{\mathrm{T}}\mathbf{Q}\overline{\boldsymbol{\Psi}} + \overline{\boldsymbol{\Psi}'^{\mathrm{T}}\mathbf{Q}\boldsymbol{\Psi}'} + \overline{\mathbf{f}} = 0, \quad (3.4)$$

where the overbar denotes a time mean, prime denotes a deviation therefrom, and $\mathbf{Q}$ is a matrix, in the same basis as $\mathbf{L}$, which contains the quadratic coefficients of the operator describing the nonlinear processes, primarily advection. Note that $\mathbf{L}$ depends on the climatological basic state (it represents a linearization around it), but $\mathbf{Q}$ does not. The two terms involving $\mathbf{Q}$ are often regarded, from the perspective of linear modeling, as ''source'' terms. The first is sometimes referred to as the ''stationary nonlinearity forcing,'' and the second is called the ''transient eddy forcing.'' Transient eddy flux convergence is seen to be important in the formation and maintenance of the equilibrium response to an SST anomaly, but the response to stationary nonlinearity, often calculated as a residual, is usually less important. Although transient eddy forcing arises from quadratic nonlinearities in the equations of motion, the anomalous transient eddy forcing need not be nonlinear in its dependence on the response to an SST anomaly (e.g., Ting 1991).

In addition to the dynamical nonlinearities in (3.4), nonlinearities in physical parameterizations can also modify the response. For example, the bulk aerodynamic formula for sensible heat flux (e.g., F85), leads to a nonlinear, flow-dependent specification of the heat flux anomaly. The anomalous release of latent heat due to an SST anomaly has an even more complex dependence on the flow. Such effects are particularly difficult to separate out, because they can influence not only the local heat flux anomaly but also the basic state, which in turn affects the linear and nonlinear dynamical responses.

The transient eddy forcing resulting from a midlatitude SST anomaly can be diagnosed from GCM calculations and then used to force a linear model [Roads 1989; Ting 1991; Ting and Peng 1995; Hall et al. 2001; see also section 4b(2)]. The result often explains much of the sometimes large differences between the full GCM response and the direct linear response to heating. In particular, the response to transient eddy vorticity fluxes can reverse the linear, near-surface response to shallow heating, replacing a baroclinic downstream low pressure anomaly with an equivalent barotropic high. The generation of a surface high pressure anomaly by an upper-level divergence of the transient eddy vorticity flux, as depicted in Fig. 5a, follows from the quasigeostrophic omega equation (e.g., Holton 1992). The eddy export of vorticity aloft is balanced by convergence, resulting in descent at midlevels, and low-level mass divergence. The vortex shrinking associated with this divergence produces the surface high pressure anomaly.

Whether the equilibrium response to an extratropical SST anomaly resembles the direct linear response to heating or is strongly modified by eddy fluxes, can depend sensitively on the climatological flow. This sensitivity is observed even in cases where the direct linear solution is largely insensitive to the basic state [Peng and Whitaker 1999; see section 4b(2)]. Moreover, when the modification by transient eddies is large, the structure of the response, as well as the dynamical balance—between eddy forcing and linear advection—that maintains it, may closely resemble that of unforced low-frequency variability [Peng and Robinson 2001; see section 4b(3)].

4. Results from forced GCM experiments

a. General comments

GCM experiments with perturbed surface boundary conditions are carried out to examine the response to SST anomalies in a more realistic context than is possible using the theoretical models described in section 3. GCMs incorporate the fully nonlinear primitive equations, including moisture advection and the parameterizations of ''physical'' subgrid-scale processes that are important to this problem, such as the turbulent surface fluxes, convection, clouds, precipitation, and radiation. Their integration is time dependent, allowing for transients on all timescales to play a role in the response. Most of these models have realistic levels of internal variability, which can easily obscure the response to external forcing. This constraint requires prudent analysis to ensure that the diagnosed responses to forcing are statistically robust (Chervin and Schneider 1976; von Storch and Kruse 1985; Pitcher et al. 1988; F85).

The major effort in the last two decades has been to reconcile two types of somewhat overlapping inconsistencies encountered in these GCM experiments. First, in most cases, the relationship between the atmospheric response identified in these experiments and the prescribed SST anomalies is different from that exhibited by observed atmosphere–ocean anomalies. This issue has been raised in theoretical studies using simpler models (section 3), and it motivated the use of GCMs in the first place (see F85). Secondly, the many different model experiments have generated disparate results that display perplexing nonlinearities with respect to the sign of the prescribed SST anomalies, their location, and the models' time-averaged state (for examples and references see Table 1). These inconsistencies cannot be explained by linear model studies, and have lead to the consideration of nonlinear processes in the interpretation of the results (see section 3c). The efforts to find consensus between different GCM studies led to repeated attempts to redesign the experiments, including the progressive deployment of more advanced models and modeling strategies, and the use of longer integrations or larger ensembles to assure robust signal detection.

The diversity in GCM modeling approaches to the extratropical response problem is reflected in our survey below. Here we divide our discussion into three parts:

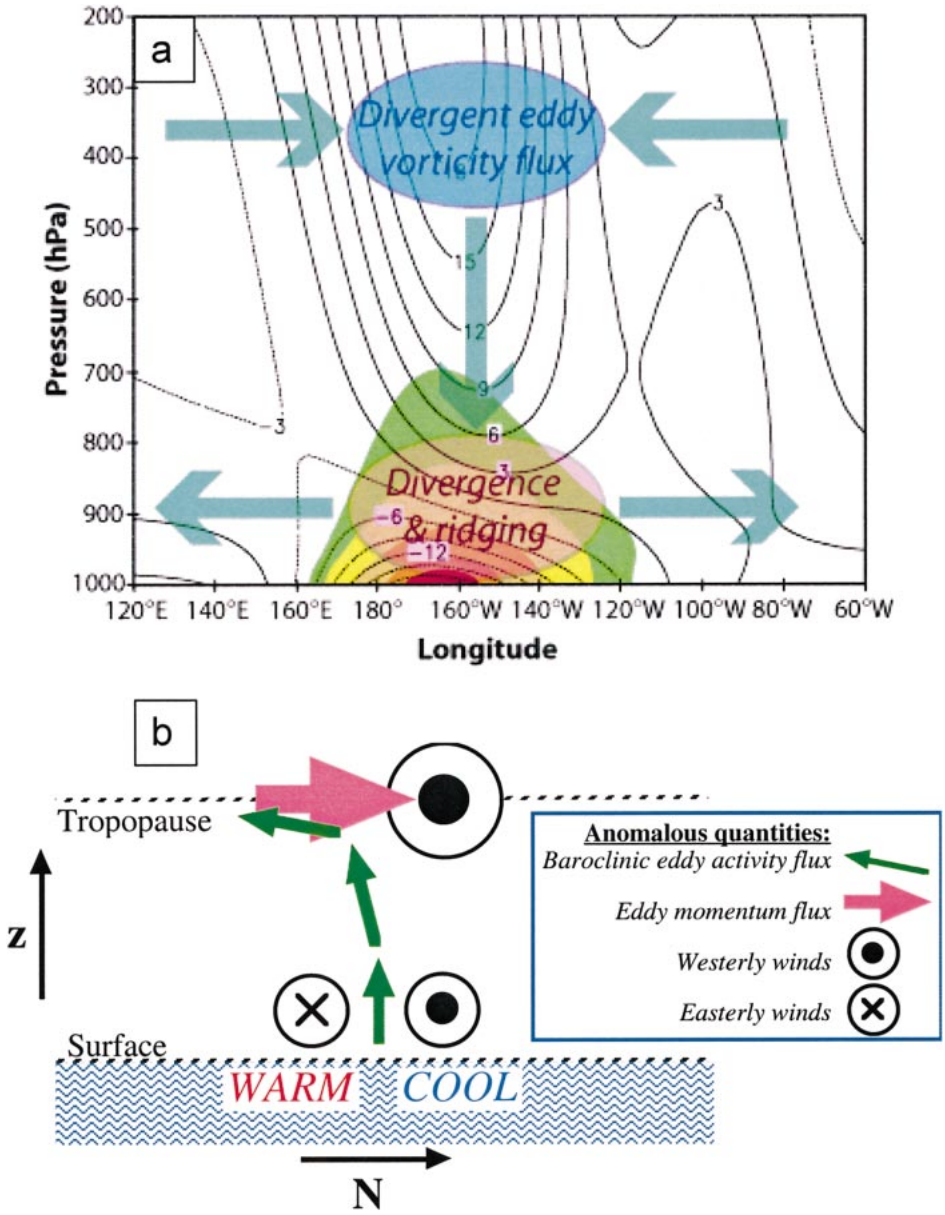

FIG. 5. Schematic diagrams that depict the role of baroclinic eddy storm tracks, in the atmospheric response to extratropical, atmosphere–ocean interaction. (a) How transient eddy vorticity fluxes (colored ellipses) and the resulting quasigeostrophic secondary circulation (wide arrows) can lead to the development of a surface ridge in response to a warm SST anomaly. The underlying colors and contours show the linear temperature and geopotential height response to shallow surface heating (see Fig. 4b). (b) The paradigm for the coupling between an oceanic response to an atmospheric low-frequency anomaly (expressed here as a dipole perturbation in the westerlies) and that same atmospheric anomaly, through the reinforcement of an anomalous storm track by the change in the surface temperature gradient [see section 4b(2) for details].

- Results from ''idealized'' GCM experiments with stationary SST anomalies that often capture only the salient features of the observed anomaly patterns such as the general location and shape, ignoring complexities such as multiple centers of activity with opposing signs (section 4b).
- Results from experiments using realistic (taken directly from observations), time-varying, SST anomalies (section 4c).
- Results from coupled models where the ocean and atmosphere components interact, creating internally consistent SST anomalies (section 5).

Despite the difficulties in interpreting extratropical SST

TABLE 1. A summary of GCM experiments with prescribed fixed SST anomalies, their properties, and their results. EqBt stands for equivalent barotropic.

Reference	SST anomaly (location and size)	Model resolution	Experimental design	Response pattern
Palmer and Sun (1985)	Western North Atlantic; 3 K	Grid point ~ 330 km with 5 levels	5 sets of 50-day runs with positive and negative SSTA, each starting with different November initial conditions	EqBt high downstream of positive SSTA; 20 m K^{-1} at 500 hPa; 1.5 hPa K^{-1} at SLP
Pitcher et al. (1988)	North Pacific; 2 and 4 K	Spectral R15 with 9 levels	Perpetual Jan; 1200-day runs with positive and negative SSTA, compared to similar control run	EqBt low downstream of both positive and negative SSTA; 25 m K^{-1} at 500 hPa; 1.2 hPa K^{-1} at SLP
Kushnir and Lau (1992)	North Pacific; 2 K (similar to Pitcher et al.)	Spectral R15 with 9 levels	Perpetual Jan; positive and negative SSTA and control each for 1350-days and 9 sets of 180-day transient runs	EqBt low downstream of both positive and negative SSTA; slow transient adjustment; 20 m K^{-1} or 2 hPa K^{-1}
Ferranti et al. (1994)	Western North Pacific and North Atlantic; 2 K	Spectral T63 with 19 levels	5 pairs (positive and negative SSTA) of 120-day runs starting with Nov initial conditions and continuing to Feb	Only 500 hPa shown; high (low) downstream of positive (negative) SSTA; 20 m K^{-1}
Peng et al. (1995)	Western North Atlantic; 3 K	Spectral T42 with 21 levels	50-day positive and negative SSTA and control runs for 6 perpetual Nov and 4 perpetual Jan cases	Downstream of positive SSTA EqBt high in Nov, but EqBt low in Jan; 30–40 m K^{-1} or 3 hPa K^{-1}
Kushnir and Held (1996)	Central North Atlantic; 4 K	Spectral R15 with 9 levels	6000-day perpetual Jan and Oct runs with positive and negative SSTA; parallel runs with idealized GCM	All runs show weak baroclinic response with surface low and upper level high downstream of positive SSTA
Latif and Barnett (1995, 1996)	North Pacific basin; 1 K	Spectral T42 with 19 levels	18-month runs with perpetual Jan conditions, positive and negative SSTA	Positive–negative composite has strong EqBt high downstream of positive SSTA; 5 hPa K^{-1} at SLP
Peng et al. (1997)	Central North Pacific; 2.5 K	Spectral T40 with 18 levels	Two cases (perpetual Jan and Feb) each has 4 pairs (positive SSTA and control) of 96-month run	Downstream of positive SSTA EqBt high (10 m K^{-1}) in Feb but baroclinic low (1 hPa K^{-1}) in Jan

experiments and reconciling the differences among them, past results suggest a set of common conclusions:

- GCM responses to extratropical SST anomalies with realistic spatial sizes and amplitudes of up to a few degrees are on the order of 10–20 gpm K^{-1} anomaly at 500 hPa. These values are in agreement with theoretical considerations and are small compared to intrinsic atmospheric variability or to the GCM response to tropical SST anomalies (e.g., Ferranti et al. 1994).
- Most GCMs exhibit a positive correlation between the upward surface flux of moist static energy and the prescribed SST anomalies, implying a damping of the latter. The rate of damping is typically, 10–20 W m^{-2} K^{-1} (e.g., Kushnir and Held 1996). In contrast, observed SST anomalies are generally driven by surface fluxes [see section 2b(1)]. Arguably, the GCM surface flux response can be seen as connected with the observed thermodynamic adjustment of the marine boundary layer temperature and humidity to the change in SST (Frankignoul et al. 1998). Some notable exceptions to this surface flux discrepency are associated with transient experiments (i.e., short integrations on the order of a month or two) that also display a strong equivalent barotropic response unlike that suggested by linear considerations (see more below).
- In GCM experiments, precipitation response to the imposed SST anomalies occurs close to the latter reflecting only a small downstream displacement due to advection. The corresponding anomalous heating profile is much shallower than the heating induced by tropical SST anomalies (e.g., Kushnir and Held 1996; Peng et al. 1997). This situation justifies the typical heating functions imposed in theoretical modeling studies (section 3).
- The most reproducible part of the response is the change in lower-tropospheric temperature, which tends to be largest near the surface and to decay rapidly with height. The change in surface temperature tends to be smaller than the imposed SST anomaly, consistent with the surface flux response (e.g., Kushnir and Held 1996; Peng et al. 1997).
- There is evidence that the response is sensitive to the model's climatological basic state and that shifts in the storm tracks play a role in the response to imposed SST anomalies (e.g., Peng et al. 1997; Peng et al. 1995).
- Coupled GCM studies, in which the ocean can respond to the changes in the atmosphere, are capable of generating joint variability in SST and the atmosphere similar to that found in observations, including the observed correlation between SST and surface fluxes. Coupled GCMs can be used in a hierarchical modeling approach (e.g., with uncoupled GCMs) to assess the significance of SST feedback on the atmosphere (e.g., Bladé 1997; Saravanan 1998; and see section 5).

b. GCM response to stationary and simplified SST anomalies

Early GCM experiments exploring the atmospheric response to extratropical SST anomalies were designed as an extension of theoretical studies, that is, they were meant to determine and to understand how the atmosphere responds to a stationary patch of unusually warm or cold ocean placed in mid- or high latitudes. Various simplifications in GCM experiments with prescribed SST anomalies were motivated by the realization that the ''signal-to-noise'' ratio in such experiments is low, and by the desire to remain close to the setting in theoretical models and thereby simplify the interpretation of the results. These simplifications generally involve one or more of the following modifications of the natural system:

- The prescribed SST anomalies are stripped of details to capture the ''essential features'' of the observed patterns, or to preserve just the extratropical portion of a more global pattern and the prescribed SST anomalies are amplified to induce a clearly detectable response pattern (e.g., Palmer and Sun 1985; Ferranti et al. 1994; Pitcher et al. 1988; Kushnir and Held 1996).
- The models are integrated in ''perpetual month'' conditions, that is, fixing the climatological SST background to that of a single calendar month, holding the solar zenith angle at that month's value, and keeping soil moisture and snow cover at their climatological values to reduce other sources of variability.

Most simplified experiments are integrated for a time much longer than a month, allowing the model atmosphere to equilibrate with the anomalous SST (e.g., Pitcher et al. 1988; Kushnir and Held 1996). Alternatively, ensembles of short experiments are executed in which the same SST anomaly is imposed but with different initial conditions, all consistent with the corresponding calendar month (Palmer and Sun 1985; Peng et al. 1995). Results are compared to ensembles of unperturbed runs or to integrations forced with the opposite sign of the same anomaly, thus potentially enhancing the signal-to-noise ratio (e.g., Palmer and Sun 1985). Kushnir and Lau (1992) suggested that the method of integration influences the response, because the adjustment of the atmosphere to the perturbed SST distribution involves timescales longer than a season.

Table 1 lists several representative studies in which atmospheric GCMs were forced with stationary SST anomalies. Despite the relatively simple experimental setting, response patterns vary considerably, from baroclinic patterns that resemble the response of linear models (Kushnir and Held 1996) to equivalent baro-

tropic patterns that, in a coupled system, could reinforce the prescribed SST anomaly (Ferranti et al. 1994; Peng et al. 1995, their November case). Significant differences are also found regarding the linearity of the response relative to the strength and polarity of the SST anomaly. Some studies show that the response, at least locally, is largely proportional to the anomaly strength (Palmer and Sun 1985) and changes sign when the sign of the anomaly is reversed (Ferranti et al. 1994), while others find that the response is nonlinear (Pitcher et al. 1988; Kushnir and Lau 1992).

To make further progress, it is necessary to understand why the model results are so diverse. This is difficult, because different studies used different GCMs forced with different SST anomalies, and employed different experimental procedures. All of these differences can contribute to the large disparity in the results. Much of the recent research in this area has been dedicated to reconciling the differences by using models with improved resolution and physical parameterization schemes and by generating larger ensembles to assure statistical reliability. From these recent experiments, three potentially related factors have emerged as important for determining the diversity in the response patterns: the underlying climatological state and its relationship to the SST anomaly, the baroclinic eddy (storm track) response to the forcing and its feedback on the large-scale flow, and the relationship between the response and the model's unforced, low-frequency variability. These results closely follow the theoretical developments described in section 3. As is detailed below, the links between the theory and the GCM results have in several instances, been strengthened using simplified dynamical models.

1) THE ROLE OF BACKGROUND CLIMATOLOGY

Peng et al. (1995, see Table 1) were the first to suggest that the response depends on the underlying model climatic state, that is, the equilibrium state that the model assumes under a given solar zenith angle and the unperturbed (climatological) SST distribution. In their study, a realistic warm SST anomaly in the western North Atlantic, near the Grand Banks, yielded drastically different responses under November and January conditions. Downstream from the prescribed SST anomaly the November response was a strong, equivalent barotropic high pressure anomaly while the January response was a somewhat weaker equivalent barotropic low. Experiments with a cold SST anomaly in the same location yielded no significant response in either month. Peng et al. (1997, see Table 1) provide further evidence for the influence of the background climatology on the model response, this time with a North Pacific warm anomaly and a different model (albeit with a similar horizontal resolution). In these North Pacific experiments, mean January and February background conditions were used. The model's mean state during these two months exhibits an unrealistically large difference in the circulation over the North Pacific, with a weaker and much more zonal flow in February than in January. Embedded in these two different mean states, the model response to the same SST anomaly exhibits a baroclinic structure with a shallow low pressure anomaly in January, and an equivalent-barotropic high in February.

The Peng et al. (1997) results could have stemmed from either a stationary nonlinearity, independent of the mean state (section 3c), or from the dependence of the linear response to the heating on the background flow (section 3b). In the next section, however, we argue that it is the difference of the storm track response given the differences in the underlying climatology, which forces different stationary anomalies in the two months, thus yielding two different patterns of response to the same SST anomaly.

2) ROLE OF BAROCLINIC EDDY FEEDBACK

As described in section 3b, the linear response to midlatitude heating in a realistic model is invariably baroclinic and is largely insensitive to the model details. There are, however, subtle differences between the responses in different basic states that could amplify through interactions with transient eddy storm tracks. Ting and Peng (1995) used an idealized heating profile in the western North Atlantic to force a model linearized about the November and January basic states of the Peng et al. (1995) GCM experiments. They found that the November upper-level high produced by the heating was located north of its January counterpart. Ting and Peng then extracted the transient eddy forcing terms from the full GCM experiments and used it to force the linear model. The combined linear response to SST-induced heating and anomalous transient eddy fluxes of momentum and heat came close to explaining the full GCM response of Peng et al. (1995). Ting and Peng (1995) stipulated that because the November jet in this GCM is more zonal than in January, the heating related to the same SST anomaly induces an upper-level response that weakens the jet in November but strengthens it in January. This, they argued, has the potential to cause a different response in the storm track, and, therefore, a different baroclinic eddy feedback on the quasi-stationary flow. However, the success in prescribing the different forcing terms from the GCM experiment in a linear model to obtain the whole does not constitute a proof to this stipulation.

Peng and Whitaker (1999) considered the competition between heating and transient eddy forcing in the response to a Pacific SST anomaly, as found by Peng et al. [1997, section 4b(1) and Table 1]. As in Ting and Peng (1995), this study makes use of a linear, time-dependent, primitive equation model to examine the separate and combined responses to heating and transient forcing taken from the GCM runs. Peng and Whi-

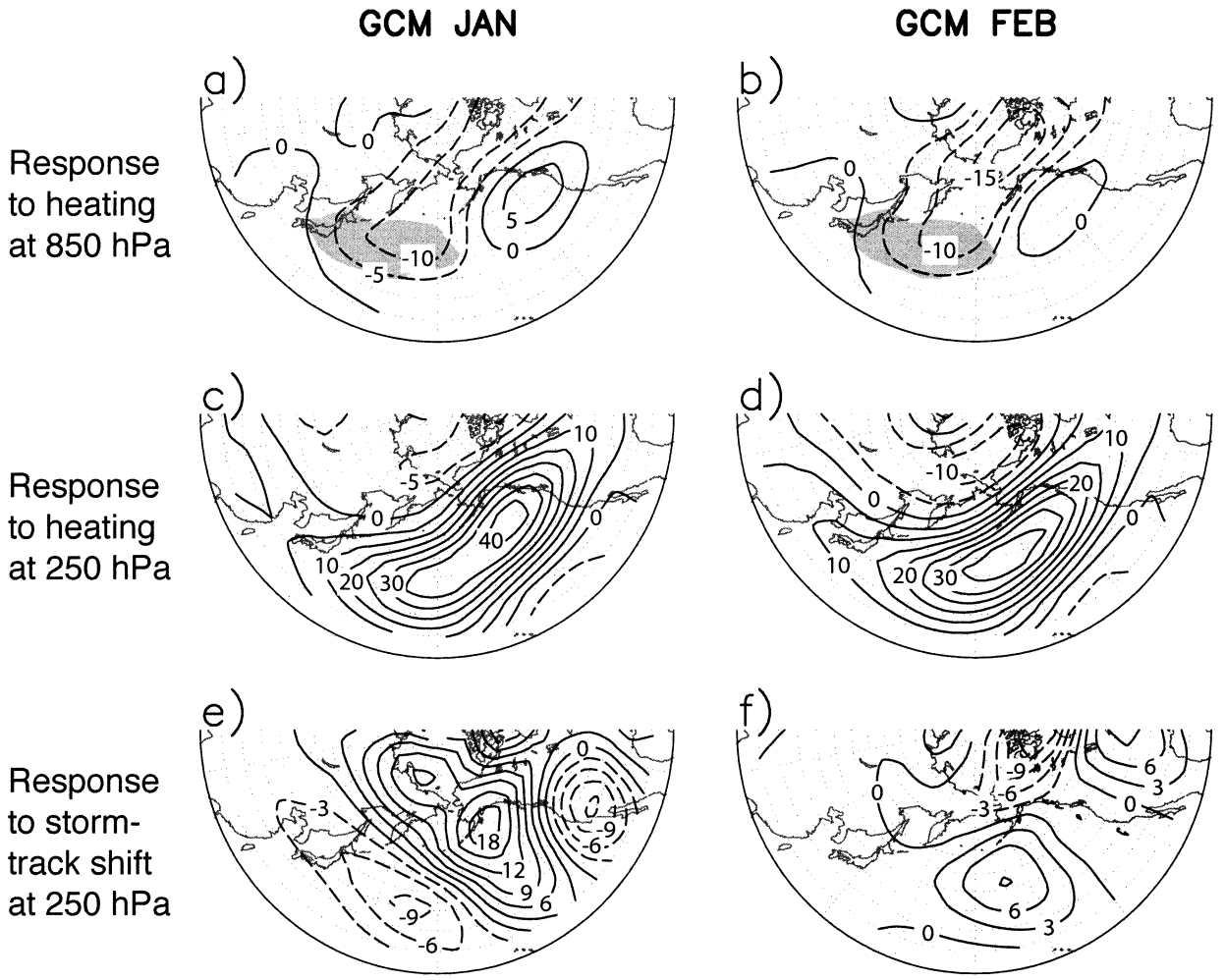

FIG. 6. A summary Peng and Whitaker linear analysis of the response to a North Pacific SST anomaly in two different climatological states, Jan and Feb, of a full GCM. (a), (b), (c), (d) The response of a linear, primitive equation model to heating corresponding to a prescribed SST anomaly in the region indicated by light shading in (a) and (b), and at the indicated levels. (e), (f) The response of the same linear model to an eddy driven, geopotential height tendency calculated by a linear storm track model, linearized around the same Jan and Feb states plus the heating perturbations shown above [see section 4b(2) for more details]. Contour interval in (a)–(d) is 5 m and in (e)–(f) is 3 m. The figure is drawn after Peng and Whitaker (1999).

taker, however, go one more step toward resolving the role of eddy interactions in the response. The linear model with the January and a February GCM basic states is forced with a heating perturbation that represents the direct effect of the SST anomaly in the full GCM. The linear responses to the heating in the two basic states are baroclinic and are very similar (Figs. 6a–d). The eddy feedback on the heating-induced anomalous flow is then simulated by constructing a new basic state that is the sum of the GCM climatological flow for each month, and the corresponding linear response to heating. This new basic state is prescribed in a linear, quasigeostrophic, storm track model. The storm track model is perturbed by stochastic forcing to estimate baroclinic eddy statistics, including the eddy vorticity fluxes that are associated with a given basic state, and this allows the calculation of the resulting geopotential height tendency (Whitaker and Sardeshmukh 1998). The geopotential height tendency from the storm track model is then used to force the linear, primitive equation model yielding the anomalous flow driven by the eddy momentum forcing. This is shown in Figs. 6e,f. The eddy-forced perturbation is equivalent barotropic in both months, but its relation to the heating response pattern is different. In January (Fig. 6e), the eddy-driven anomalous flow shifts the heating-induced upper-level high northeastward, and the surface low is somewhat reinforced. However, in February (Fig. 6f), the eddy forcing at the center of the North Pacific basin is in the same sense as the upper-level high, produced by the heating. At the surface the eddy forcing acts to reverse the sign of the response to heating. These results confirm that the source of the weak surface high and the equivalent

barotropic response in February, is eddy feedback that counteracts the baroclinic response to the SST-induced heating, as schematically depicted in Fig. 5a.

The picture emerging from the Peng and Whitaker analysis suggests a paradigm for an eddy-mediated interaction between low-frequency atmospheric variability and SST-forced anomalies in nature, where SST is responding to atmospheric forcing. The paradigm is depicted in Fig. 5b: a change in SST, forced by an equivalent-barotropic perturbation in the atmosphere, creates an anomalous SST and surface temperature gradient that drives an anomalous storm track. The eddy activity emanating from the anomalous track behaves just like its counterpart in the climatological circulation. In the upper troposphere, it causes a convergence of the eddy momentum flux that reinforces the low-frequency perturbation. The secondary circulation responds to this upper-level change by inducing a change in the same sense in the lower troposphere. Thus, the entire perturbation is enhanced. This relationship between the perturbations in the jet and in the storm track could occur in nature without a change in SST, because it is characteristic of low-frequency variability in the extratropical atmosphere (e.g., Lau and Nath 1991). In this paradigm, however, we propose, based on the GCM experiments described above, that the SST response to atmospheric forcing provides weak but positive reinforcement to this internal atmospheric process.

Eddy feedback has been shown to depend not only on the storm track climatology but also on the position of the heating (or SST anomaly) relative to the storm track. With heating over the western North Pacific, synoptic eddies provide a strong positive feedback, favorable for developing an equivalent-barotropic ridge. When the heating is shifted to the eastern Pacific, the eddy feedback is drastically different (Peng and Whitaker 1999). This is consistent with theoretical work described in section 3 (Hall et al. 2001; see also Walter et al. 2001). Together these studies suggest that eddy feedback depends on the configurations of the climatological storm track, the SST anomaly (heating), and their relative positions. Hence, changes in either the storm track climatology or the SST anomaly can result in different eddy feedbacks and eventually different equilibrium responses. Moreover, eddy feedback can conceivably lead to asymmetric responses as the sign of the SST anomaly is reversed. Eddy momentum fluxes thus appear to play a significant role in both modulating and maintaining the responses to surface heating anomalies in GCMs and, presumably, in nature.

3) Relationship to intrinsic model variability

Peng and Robinson (2001) examined the relationship between the SST-forced response from Peng et al. (1997, see Table 1) and the model's unperturbed internal variability. This comparison suggests that the SST-forced response comprises a local and direct linear response to low-level heating and an eddy-driven component [see section 4b(2)] that closely resembles patterns of the model's internal variability. The former is baroclinic and the latter equivalent barotropic, extending over the entire hemisphere. The barotropic part of the response is manifested as a change in the probability distribution functions (PDFs) of the leading EOFs of monthly 500-hPa anomalies. From this, Peng and Robinson concluded that in order for a warm SST anomaly over the western North Pacific to induce an equivalent-barotropic high in the center of the basin, the model's internal variability must have a well-defined center of action there. Because unperturbed perpetual January and February simulations with this model have very different patterns of internal variability, this argument provides another explanation for the different responses to an SST anomaly in the two months.

The interpretation of extratropical SST anomalies as an agent for shifting the frequency of the modes of unforced variability or for affecting their intensity is appealing, as it fits well with ideas about the chaotic behavior of the extratropical atmosphere, but it also leads to difficulties in detecting the signal of the response to an SST anomaly. Proving that the multivariate PDF of the model variability is significantly different in two different realizations is much more difficult than proving that the mean climates of these realizations are different. An apparent change in the distribution of model variance between of leading EOFs in response to an extratropical SST anomaly may be only the signature of insufficiently sampled internal variability (Cheng et al. 1995).

Another consequence of the apparent relationship between the response to SST forcing and internal variability is that a model that does not represent well the patterns of atmospheric variability cannot adequately represent the response to extratropical SST anomalies. More generally, the quality of a model's simulation of the climatological flow, its simulation of transient eddy fluxes, and its simulation of internal low-frequency variability are tied together, and together they influence a model's response to SST anomalies. It is noteworthy, then, that GCMs often deviate significantly from the atmosphere in all three respects (e.g., Roeckner et al. 1992, 1996; Peng and Robinson 2001).

Peng and Whitaker (1999) found that the eddy-modulated response to North Pacific idealized heating was significantly greater when the observed winter climatology was used as the basic state for their linear and storm track models, instead of that from their GCM. Similarly, Peng and Robinson (2001) found that the statistical association between low-level warmth and an equivalent barotropic ridge was much stronger in observations than in the GCM. These results are hard to interpret, but they suggest that models could be underestimating the dynamical response to SST anomalies by as much as a factor of 2.

c. *Response to time-varying SST variability in ''realistic'' model integrations*

While much has been learned from experiments in which atmospheric models are forced with idealized time-independent SST anomalies, the real SST field varies continuously in both space and time, as does the climatological state of the overlying atmosphere. This complexity needs to be engaged if model results are to be relevant to the natural system. One strategy that has proved fruitful is to force an atmospheric model with the observed history of SST variations. This approach, pioneered by the Atmospheric Model Intercomparison Project (AMIP; Gates 1992), holds the attraction that one can directly compare model results with the observed atmospheric evolution.

This section brings together insights from AMIP-type studies that are relevant to understanding the atmospheric response to extratropical SST anomalies. Two points should be appreciated at the outset, however. First, in the great majority of such studies the models have been forced with ''global'' SST anomalies. The influence of extratropical SST anomalies is therefore blended with, and often dominated by, the influence of tropical SST anomalies (Lau and Nath 1994; Graham et al. 1994). Separating these influences is difficult, if not impossible, unless parallel experiments are conducted in which SST anomalies are prescribed only in the extratropics. Second, in very few AMIP-type studies has there been substantial attention focused on the mechanisms associated with the response to SST variations. Rather, the major relevant contribution of this body of work has been in quantifying the relative importance of internal and SST-forced variability, and in characterizing certain basic features of the latter. The discussion will therefore focus on these aspects, specifically on the analyses of ''potential predictability''—a measure of the relative importance of internal and forced variability—and the space–time characteristics of the SST-forced variability.

1) POTENTIAL PREDICTABILITY

That the variance of the extratropical atmosphere arising from internal processes is large in comparison with the variance that arises in response to SST anomalies is a theme running throughout this review. One of the most useful results of AMIP-type studies has been the quantification of the relative importance of these two influences when SSTs vary realistically. Several authors (e.g., Lau 1985; Harzallah and Sadourny 1995; Kumar and Hoerling 1995; Zwiers and Kharin 1998; Rowell 1998) have employed analysis of variance (ANOVA), or a similar approach, to partition the total variance into internal and SST-forced components (more strictly, the boundary-forced component, where the boundary forcing includes variations in sea ice extent). The ratio of the SST-forced variance to the total variance is often termed the potential predictability (Madden 1976, 1983; Shukla 1983; Zwiers 1987; Rowell 1998), meaning the level of predictability that could be achieved given perfect knowledge of the boundary conditions.

In these ANOVA analyses of potential predictability, the gross structure is a striking tropical–midlatitude contrast. A typical example based on experiments with the ECHAM3.5 GCM (Roeckner et al. 1992) following the work of, for example, Harzallah and Sadourny (1995) and Rowell (1998), is shown in Fig. 7. In much of the tropical belt, particularly during winter, the SST-forced variance is 60%–80% of the total. In the mid- and high latitudes, the SST-forced variance is generally about 20% of the total, except over the eastern North Pacific during winter, when the ratio reaches 60%. The extratropical SST-forced variance, however, includes variability in the extratropics due to tropical SST anomalies, because SST anomalies are prescribed over the entire globe. In the eastern North Pacific, it is most likely ENSO influence that contributes to the ''predictable'' signal. While detailed features of these patterns vary between models, the contrast between the Tropics and higher latitudes is robust (Zwiers and Kharin 1998). This result illustrates that, while interannual variability in the tropical atmosphere is highly constrained by SST variations, the corresponding variability in the extratropical atmosphere is not.

2) SPACE–TIME STRUCTURE OF THE RESPONSE TO SST VARIATIONS

In order to identify to which aspects of the SST the atmosphere is most sensitive the space–time characteristics of the SST-forced variability must be determined. Various techniques for so doing have been applied to AMIP-type integrations. The simplest is to construct composites based on some chosen SST indices. For example, Figs. 1c,d show the results of a regression between the mean of an AMIP ensemble and the SST indices used to construct Figs. 1a,b (the variability in the model's SST is, by definition, the same as in the observations). Note that in the North Atlantic basin (Fig. 1c), only a weak expression of the strong, coherent SST–flux–wind relationship found in observations (Fig. 1a) appears. Particularly interesting is the ability of the ensemble average to create an impression of the cyclonic anomaly centered on the Azores when SST is warm in the subpolar gyre and cold in the subtropics (30°N). The pattern is far less coherent than the observed one, and in some regions the SST anomaly is weakly damped by surface fluxes. In contrast, the Pacific basin (Fig. 1d) SST–flux–wind relationship is similar to that observed (Fig. 1b) in its pattern, coherence, and intensity. The obvious caveat here is that the observed and modeled Pacific pattern is directly related to the forcing of the entire basin by equatorial Pacific SST (ENSO) and much less, if at all, to the existence of the extratropical SST anomaly (see Alexander et al. 2002, this issue).

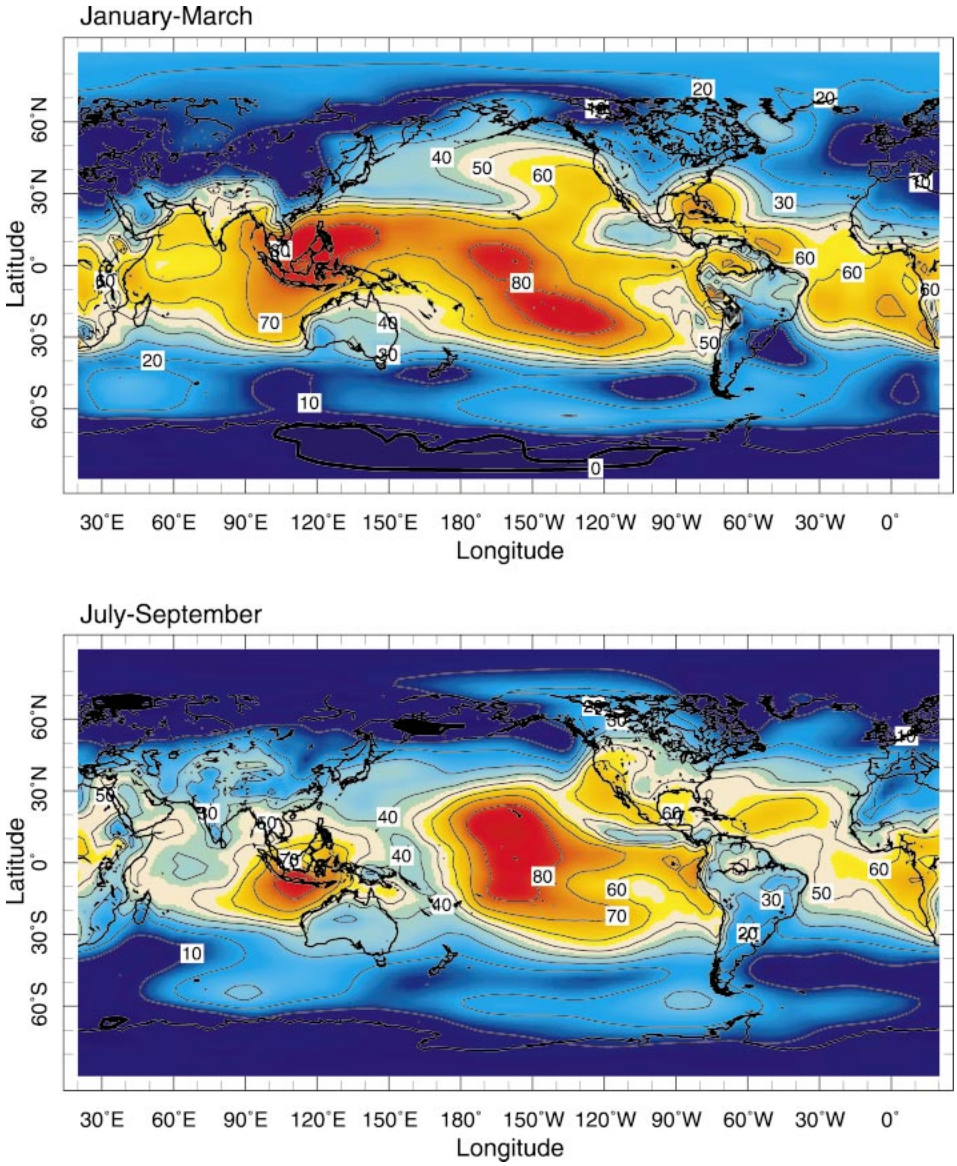

FIG. 7. Ratio of SST-determined SLP variance to total variance (or potential predictability) during winter (Jan–Mar) and summer (Jul–Sep) as determined from an ensemble of 10 GCM integrations forced with global SST and sea ice distribution 1950–99. The analysis is based on data from the ECHAM3.5 GCM provided by L. Goddard. Contours every 10%.

The use of an SST index, as demonstrated above, is appropriate when one has a good reason to expect a priori a response to a particular feature in SST, and when high signal-to-noise levels are anticipated. It has been widely used to study the atmospheric response to ENSO (e.g. Trenberth et al. 1998). In the extratropics, however, there is no consensus about which features of the SST field elicit the strongest atmospheric response. Therefore, other methodologies are required for addressing this issue objectively. The main techniques that have been used are varieties of the EOF analysis, including its cousins, singular value decomposition (SVD) and canonical correlation analysis (CCA) (e.g., Bretherton et al. 1992).

When such methods are applied to the mean of an ensemble of model integrations, the contribution to the ensemble mean variance from internal variability must be taken into account. For small ensembles, this contribution can be large, and may dominate the SST-forced signal. In such cases, the first EOF of the ensemble mean, for example, may resemble the dominant mode of internal variability and, so, offer little information about the forced signal. Steps must therefore be taken to limit or remove the effects of this ''contamination.''

Harzallah and Sadourny (1995), Ward and Navarra (1997), and Venzke et al. (1999) offer methods by which this may be done.

Attempts to identify SST-forced variability over the North Pacific invariably pick out a Pacific–North American (PNA)-like remote response to ENSO as the dominant signal (e.g., Harzallah and Sadourny 1995; Zwiers et al. 2000; and references therein). Over the North Atlantic, Venzke et al. (1999) showed that a remote response to ENSO is the dominant influence, but they also found evidence that a tripolar pattern of North Atlantic SST anomalies (as in Figs. 1a and 1c) exerts a significant influence in winter and spring. The response is characterized by a basin-scale north–south dipole in sea level pressure, associated with anomalous westerly winds around 50°–60°N, quite similar to the observed relationship (suggesting that the weak resemblance between Figs. 1c and 1a is indeed caused by the SST forcing).

Rodwell et al. (1999) suggested that a similar tripolar pattern of SST anomalies was the forcing for potentially predictable fluctuations in the North Atlantic Oscillation (NAO) index in their ensemble of AGCM simulations. They showed that the ensemble mean NAO index was well correlated with the observed NAO, a result which Mehta et al. (2000) reproduced using a different model. At first sight, these findings might appear to suggest that the NAO is strongly constrained by the SST. Such a conclusion would be at odds with the results from potential predictability studies that indicate low signal-to-noise in the North Atlantic region. Bretherton and Battisti (2000) have, however, proposed a straightforward solution to this apparent contradiction. They argue persuasively that the high correlation is a consequence of the ensemble averaging, which filters out the uncorrelated variability in the different ensemble members and enhances the signal-to-noise ratio. It does not however imply high signal-to-noise in any single realization (see additional discussion in section 5a).

The discussion up to this point has focused on the mean response to SST variations. It is, however, possible that a response could be manifested more strongly in other statistics such as a change in the variance. Robertson et al. (2000) compared a 30-yr GCM control integration forced with climatological SST and an integration forced with observed SST in the Atlantic region. He found that the latter had significantly more variance, including a fivefold increase in the variance of an NAO index. Watanabe and Kimoto (1999) also found a selective enhancement in the variance of the NAO in a similar experimental scenario. In both studies tropical, rather than extratropical, SST anomalies appeared to be primarily responsible for the enhanced variance, but further investigations are needed to understand the mechanisms involved.

5. Coupled model studies of the extratropical interaction

As stated in the introduction and in section 2, extratropical SST variability generally arises in response to fluctuations in surface heat fluxes driven by atmospheric variability. The success of ocean models in hindcasting the temporal evolution of SST anomalies when forced with observed surface atmospheric data also suggests that the prime direction of forcing is from the atmosphere to the ocean (e.g., Haney 1985; Battisti et al. 1995; Seager et al. 2000). The back-interaction exerted by these SST anomalies on the atmosphere may be misrepresented (or even differ fundamentally) in the one-way forcing that takes place in GCM experiments with prescribed SST anomalies (consider, e.g., the fact that in the observed, two-way interaction the SST anomaly strength and location is consistent with the atmosphere's internal variability, but this is not generally the case when observed SST anomalies are prescribed in a GCM). The two-way interaction that occurs in nature can be captured in a coupled model setting, in which the simultaneous evolution of the atmosphere and ocean are simulated and in which conditions at their interface vary interactively, as dictated by dynamical and thermodynamical constraints. The challenges in such an approach are in teasing out the ocean's contribution to the interaction, for a coupled model is almost as complex as the real world. An intelligent use of a coupled model, for example, in the context of a hierarchy of experiments with uncoupled models, can alleviate this problem. Before we review results from coupled GCM studies, we first introduce a simple framework, recently proposed by Barsugli and Battisti (1998, hereafter BB98), for understanding the thermally coupled, extratropical, atmosphere–ocean system.

a. The thermally coupled system

Consider the simplest model of atmosphere–ocean interaction, in which the temporal evolution of SST depends only on the local fluctuations in surface heat flux due to atmospheric variability and in which the atmosphere responds to changes in SST. To capture this behavior, BB98 proposed a modification of the linear, one-dimensional, stochastic model of Frankignoul and Hasselmann (1977; see also F85) in which the interaction is one way. In the BB98 linear model, the SST anomaly tendency depends (following a linearized version of the bulk formulas and radiative cooling) on the anomalous atmospheric column mean temperature (the surface air temperature anomaly is assumed to be proportional to the column mean temperature anomaly) and on the SST anomaly. These dependences are linear: the atmosphere term is forcing and the SST term is damping. The atmospheric column mean temperature anomaly is also affected by the surface flux, which is cooling the atmosphere when SST is warmed and vice versa. In BB98, this dependence is combined with the radiative cooling of the column. Thus, for the atmosphere, the term that depends on atmospheric temperature is damping. Forcing is provided by a term proportional to the SST anomaly (reflecting the heat flux exchange) and a stochastic

(white noise) term representing the effect of internal atmospheric dynamics on the column mean temperature anomaly. The model also represents the dynamical atmospheric response to SST through an additional linear dependence of atmospheric temperature tendency on the SST anomaly. Accounting for the large difference in heat capacity of the atmospheres and the oceanic mixed layer allows the model to represent the large differences in the adjustment timescales of the two components.

The physics described above is captured in two simple, nondimensional, linear equations, one for the rate of change of atmospheric temperature anomaly and the other for the SST anomaly:

$$dT_a/dt = -aT_a + bT_o + N(t) \tag{5.1}$$

$$\beta dT_o/dt = cT_a - dT_o. \tag{5.2}$$

Here N is the random (white noise) process representing the effect of internal atmospheric variability; β is the ratio between oceanic mixed layer and atmospheric heat capacities. Parameters a and d are the damping coefficients that include the effects of radiative cooling and surface fluxes; c is the coefficient of proportionality between surface air temperature and free air temperature. The second term in the atmospheric temperature equation (5.1) is a combination of the thermal forcing due to SST, T_0, and the dynamical forcing of the atmosphere by the SST, expressed as $(b - 1)T_0$. The dynamical response is estimated by BB98 from coupled GCM experiments, where it was found to partially offset the thermal effects of an SST anomaly, that is, $0 < b < 1$. The system is stable for $ad > bc$. Of those four parameters b is the least well known and, judging from the discussion in section 4, it can vary greatly from one GCM to another. In their analysis BB98 chose $b = 0.5$, $a = 1.12$, $d = 1.08$, and $c = 1$.

The linearity and simplicity of the BB98 model makes it is easy to calculate the Fourier transforms of air temperature and SST, their specta and autocorrelation functions, as well as the spectrum of surface heat flux (see BB98 for details). By explicitly calculating the surface heat flux and its contribution to atmosphere and ocean temperature tendency, the BB98 model clearly distinguishes between forcing and damping. This separation allows for direct comparison of different types of GCM experiments coupled and uncoupled and assess the effect of thermal coupling on SST and atmospheric temperature variability. In their investigation BB98 looked at the following scenarios:

- A fully coupled system as described in the first paragraph of this section.
- An uncoupled system in which the atmosphere responds only to its internal dynamical noise, $b = 0$, and the ocean is forced with the resulting air temperature in a diagnostic mode.
- A system in which the atmosphere is forced with prescribed time-varying SST anomalies, just as in the AMIP GCM runs described in section 4b. To simulate such a system, SST anomalies from a separate run of the fully coupled system are used to force the atmosphere temperature equation (through the surface heat flux and linear response terms) in addition to stochastic noise forcing.

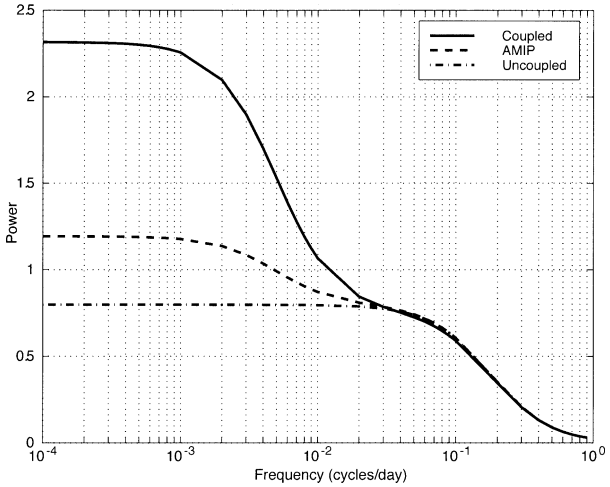

FIG. 8. The spectra of atmospheric temperature in the Barsugli and Battisti (1998) linear, one-dimensional model, in its coupled, "AMIP," and uncoupled versions. The frequency is given in units of day^{-1}.

Using this approach BB98 showed that coupling enhances the variance and persistence of both the atmosphere and ocean temperatures. The increase in atmospheric variance due to the coupling is significant (Fig. 8) but becomes noticeable only on interannual timescales. The increase in atmospheric persistence is modest compared to that of SST (see BB98). BB98 also showed that air–sea coupling decreases the surface heat flux between the ocean and the atmosphere, and that, in experiments with prescribed SST anomalies, the heat flux at low frequencies is likely to be too large and of the wrong sign. This result is consistent with the unrealistic SST flux correlation found in GCM experiments with prescribed SST (section 4a) and it also suggests that such experiments will tend to underestimate the variance of atmospheric low-frequency variability.

One way to interpret the effect of atmosphere–ocean coupling is to consider the reduction in the thermal damping exerted by the ocean on the atmosphere as the former responds to variations in the surface heat flux. When the SST anomalies are kept fixed at their climatological value, thermal damping is large on all timescales. Moreover, if an atmospheric perturbation is equivalent barotropic, the influence of this thermal damping on it extends to all layers of the troposphere. This effect was illustrated by Hendon and Hartmann (1982), who showed that the inclusion of a sensible heat flux (negatively proportional to surface air temperature) acts as a strong damping on the extratropical atmospheric response to tropical diabatic heating. In a coupled scenario, for timescales longer than the decorre-

lation time of the mixed layer temperature (i.e., a few months), surface thermal damping decreases as the ocean temperature adjusts to the atmospheric perturbation, particularly at very low frequencies for which the oceanic adjustment is nearly complete. The result of this ''*reduced thermal damping*,'' as this mechanism is now commonly known, is a local enhancement in the low-frequency low-level atmospheric thermal variance. Persistent and equivalent barotropic perturbations should ''feel'' this effect throughout the troposphere.

An analogous linear, stochastic model was formulated by Saravanan and McWilliams (1998) to explain decadal variability. Their model adds an ocean advection term to the local thermodynamical coupling captured in the BB98 equations. When spatially coherent atmospheric low-frequency variability overlies a region where slow oceanic temperature advection is present, stochastic forcing can yield a peak in the SST spectrum at a frequency determined by the spatial scale of the low-frequency atmospheric anomalies and the advecting velocity in the ocean. Given some coupling between ocean and atmospheric temperatures, this peak imprints itself weakly on the atmosphere. Another way to extend the BB98 model to the decadal timescale was proposed by Czaja and Marshall (2000).

Further use of the BB98 model was made by Bretherton and Battisti (2000) to put into context the NAO predictability studies of Rodwell et al. (1999) and Mehta et al. (2000). As indicated above [section 4c(2)], these experiments show surprising ensemble mean skill in reproducing the NAO variability on interannual timescales when forced with a time history of observed SST anomalies. While it is tempting to conclude that there is predictability associated with the oceanic state, Bretherton and Battisti show that the same ensemble mean skill is obtained when the BB98 model is run in AMIP mode. Yet, in this case, all variability is ultimately driven by unpredictable atmospheric noise. They explain this result by noting that the observed SST anomalies used to drive the GCM integrations result from nature's own integration of one particular realization of atmospheric noise. In the mean of a large ensemble of GCM runs forced with such SST anomalies, the model-generated high-frequency variability is filtered out leaving a low-frequency atmospheric response that reflects the weak influence of SST variability common to all members of the ensemble. Thus, they argue, the reproduction of atmospheric variability in a hindcast ensemble experiment does not imply predictability. In a coupled system, the atmosphere continually forces the SST and, despite the latter's persistence information is lost in a season or so (about the damping timescale of the SST anomaly). This rate of decay determines the limit of predictability for the extratropical system. Moreover, while the variability in the forced ensemble mean is reasonably well correlated with observations, its amplitude is reduced considerably (in the BB89 model the variance is reduced by the numerical value of the damping to forcing ratio—*ad*/*bc*, see above). Palmer (1995), who discusses the coupled extratropical interaction in a different context, also suggests that if the role of the midlatitude oceans in climate is tantamount to a ''storage'' or ''capacitor'' heat device, then it cannot lead to a significant enhancement in predictability.

b. Results from coupled GCM experiments

The influence of extratropical SST anomalies on the atmosphere in coupled models has generally been assessed by comparing the atmospheric variability of the coupled midlatitude system with the uncoupled variability that develops in the presence of climatological SST conditions (Schneider and Kinter 1994; Gallimore 1995; Barsugli 1995; Manabe and Stouffer 1996; Delworth 1996; Lau and Nath 1996; Bladé 1997, 1999; Bhatt et al. 1998; Saravanan, 1998). The atmospheric models in these studies ranged from an idealized two-level zonally symmetric model to full GCMs with high resolution ($\sim$2.5°). The ocean component in these models varied from a motionless slab mixed layer to a full ocean model. Yet, all of these experiments reached the same conclusion: consistent with the linear, one-dimensional model of BB98, they all indicated that coupling to the midlatitude oceans increases the low-frequency atmospheric thermal variance and extends the persistence of atmospheric anomalies.

The dependence of this increase on the timescale of the variability was demonstrated by, for example, Manabe and Stouffer (1996) and Bladé (1997). Manabe and Stouffer, examined the enhancement of surface-temperature variance during coupling to an ocean model and showed that the enhancement is practically the same when a full ocean model and a simple 50-m-deep slab mixed layer are used. These results suggest that the bulk of the impact of air-sea coupling is due to thermodynamic effects alone. For annual timescales, the increase in the variance of surface atmospheric temperature, averaged over the midlatitude oceans, is on the order of a factor of 2, which is qualitatively consistent with the estimates in Bladé (1997), Bhatt et al. (1998), or even in Barsugli's (1995) simple two-level model. The accompanying increase in upper-tropospheric variance should be smaller. In Bladé's perpetual January experiments, the total variance of 90- and 300-day mean 500-hPa height increases by merely 10% and 20%, respectively.

Through the weak, positive (albeit passive) feedback associated with reduced thermal damping, coupling can increase the persistence of those atmospheric structures that are most sensitive to this damping (BB98 term this effect ''selective enhancement''). This effect can cause a slight reordering of the variance among the principal modes of variability (Saravanan 1998; Bladé 1999) without a substantial modification of their spatial structure. Indeed, even in high-resolution atmospheric GCMs coupled to full dynamical ocean models, these structures

exhibit only minor modifications compared to those in the uncoupled models (Delworth 1996; Barnett et al. 1999).

The reduced thermal damping effect should be considered as the baseline or null hypothesis for any coupled versus uncoupled model comparison, or when testing for the presence of decadal variability. It has yet to be determined if more active types of coupled interactions, in which the ocean and atmosphere participate in a sequence of positive and negative feedbacks leading to climate oscillations (e.g., Latif and Barnett 1994), occur in nature. The signature of such interactions would be a lag–lead correlation between the free atmosphere and SST that is either closely symmetric about lag zero or stronger when the ocean leads (BB98). Advective processes in the ocean could also potentially result in nonlocal coupling (e.g., Saravanan and McWilliams 1998, discussed in section 5a). Because of the slow oceanic timescales, however, these would be important only at decadal timescales.

6. Conclusions: The emerging picture

In writing a review such as this, the authors make an implicit contract with the reader that enough progress has been made in a field of study that it can be considered a body of knowledge. So, what can we say we know about the atmospheric response to the extratropical ocean, and, specifically what new knowledge has been developed in the 16 years since Frankignoul's review?

First, we can now say with confidence that the extratropical ocean does indeed influence the atmosphere outside of the boundary layer, but that this influence is of modest amplitude compared to internal atmospheric variability. Taking a linear perspective, we can think of the response as scaling with the strength of the SST anomaly, and ask, how many meters of geopotential perturbation do we expect for each degree of SST anomaly? A reasonable value for this parameter is 20 m K^{-1} at 500 hPa, though deficiencies in model climates and variability may weaken the response. A response of this size is also consistent with the absence of a robust, extratropical SST-forced signal in atmospheric observations, and with the fact that atmospheric models forced with climatological SST do not appear to be significantly deficient in their interannual variability.

Second, we now possess an improved understanding of the dynamics of the atmospheric response. It is recognized that transient eddies are crucial in shaping the response, and, that the resulting response patterns project strongly on internal modes of variability that are similarly governed by interactions between the transients and the large-scale flow. This result is relevant to all external forcing of the midlatitude climate. Because the internal variability is so vigorous, its dynamics are likely to dominate the responses to all but the strongest forcing. Hence, the direct linear response to any forcing will rarely be relevant in the extratropics. Rather, responses must necessarily be sought in potentially subtle changes in the probability distributions of internal modes of variability.

Third, a much clearer picture of the behavior of the coupled atmosphere–ocean system has emerged. Perhaps most revealing is the remarkable ability of a linear stochastic model to explain the behavior and predictability of a complex coupled nonlinear system. The Barsugli and Batistti (1998) model is of practical use for interpreting the results of experiments with various flavors of Arctic Oscillation (AO) coupling. This simple model demonstrates, consistent with results from coupled GCM experiments, that the dominant influence of the midlatitude ocean on the overlying atmosphere is to reduce the thermal damping of atmospheric low-frequency variability. The reduction is especially noticeable when the longest timescales are considered. In this respect, we must, however, consider that the link between surface and midtropospheric air temperature assumed in BB98 may in part be communicated from the surface up by the effect of eddy–mean flow interaction as discussed in section 4b(2). In addition, the striking success of the linear stochastic model in reproducing and explaining the results of AMIP experiments suggests that, while there may indeed be interesting dynamical nonlinearities lurking in the system, they are not central to its behavior.

A final question that must be addressed in any review such as this regards the outlook for the future. While surprises are, by definition, not foreseeable, we would be surprised indeed by any development that revealed a much larger response to extratropical SST anomalies, or a more dominant role for this response in the variability of the extratropical atmosphere, than that described above.

We expect that the most interesting future research will address how the relatively weak, but not zero, influence of the ocean on the overlying atmosphere, together with the very strong influence of the atmosphere on the ocean, determines the variability of the extratropical, coupled system. Of particular interest is the influence of SST anomalies during the transition seasons, fall and spring, when atmospheric internal variability is reduced but the mechanisms of eddy–mean flow interaction and reduced thermal damping are still relevant. We suggest that it is in this time of the year that knowledge of the SST is most likely to help in extended-range prediction. One way to proceed is through the consideration of seasonal-to-interannual predictability, using large ensembles of experiments in a coupled system. Such experiments can be used to explore how reemergence affects atmospheric variability in the fall and early winter, and how the eddy-mediated reinforcement of low-frequency variability affects persistence during late winter, when the SST anomalies are strong.

It is also important to assess the potential contribu-

tions of extratropical atmosphere–ocean interaction to long-term persistence and decadal variability, which are observed in the North Atlantic and North Pacific basins. A judicious use of coupled and uncoupled models, including experiments in which SST variability is prescribed over some parts of the ocean while allowed to be interactive in others can help in this research. Long integrations will be needed and analyses should consider changes in the probability distribution of atmospheric variability, rather than seeking a deterministic answer.

Acknowledgments. The authors wish to thank many colleagues who helped through discussion or by reading and commenting on a previous version of this review. Particular thanks go to Isaac Held and Gabriel Lau of GFDL who through their leadership in the GFDL–University Consortium initiative, facilitated model experiments, their analysis, and the discussion of the results that formed the basis for much of this review. Thanks also go to Richard Seager of LDEO who was a continuous source of skepticism, debate, interpretation, and ideas to YK and WR. We thank J. Miller for assistance in the analysis of observational and model data. Finally, we thank three anonymous reviewers who provided insightful comments on an earlier version of this manuscript and helped improve its presentation. YK acknowledges support from NOAA Grants UCSIO-10775411D/NA47GP0188 and NA06GP0567. WR acknowledges the support of NSF under Grant ATM-9903503.

REFERENCES

Alexander, M. A., C. Deser, and M. S. Timlin, 1999: The reemergence of SST anomalies in the North Pacific Ocean. *J. Climate,* **12,** 2419–2433.

——, I. Bladé, M. Newman, J. R. Lanzante, N.-C. Lau, and J. D. Scott, 2002: The atmospheric bridge: The influence of ENSO teleconnections on air–sea interaction over the global oceans. *J. Climate,* **15,** 2205–2231.

Barnett, T. P., 1981: On the nature and causes of large-scale thermal variability in the central North Pacific Ocean. *J. Phys. Oceanogr.,* **11,** 887–904.

——, and R. C. J. Somerville, 1983: Advances in short-term climate prediction. *Rev. Geophys.,* **21,** 1096–1102.

——, and Coauthors, 1994: Forecasting global ENSO-related climate anomalies. *Tellus,* **46A,** 381–397.

——, D. W. Pierce, M. Latif, D. Dommenget, and R. Saravanan, 1999: Interdecadal interactions between the tropics and midlatitudes in the Pacific basin. *Geophys. Res. Lett.,* **26,** 615–618.

Barsugli, J. J., 1995: Idealized models of intrinsic midlatitude atmosphere–ocean interaction. Ph.D. thesis, Department of Atmosphere Science, University of Washington, 189 pp.

——, and D. S. Battisti, 1998: The basic effects of atmosphere–ocean thermal coupling on midlatitude variability. *J. Atmos. Sci.,* **55,** 477–493.

Battisti, D. S., U. S. Bhatt, and M. A. Alexander, 1995: A modeling study of the interannual variability in the wintertime North Atlantic Ocean. *J. Climate,* **8,** 3067–3083.

Bhatt, U. S., M. A. Alexander, D. S. Battisti, D. D. Houghton, and L. M. Keller, 1998: Atmosphere–ocean interaction in the North Atlantic: Near-surface climate variability. *J. Climate,* **11,** 1615–1632.

Bjerknes, J., 1959: The recent warming of the North Atlantic. *The Atmosphere and Sea in Motion,* B. Bolin, Ed., Rockefeller Institute Press and Oxford University Press, 65–73.

——, 1964: Atlantic air–sea interaction. *Advances in Geophysics,* Vol. 10, Academic Press, 1–82.

Bladé, I., 1997: The influence of midlatitude ocean–atmosphere coupling on the low-frequency variability of a GCM. Part I: No tropical SST forcing. *J. Climate,* **10,** 2087–2106.

——, 1999: The influence of midlatitude ocean–atmosphere coupling on the low-frequency variability of a GCM. Part II: Interannual variability induced by tropical SST forcing. *J. Climate,* **12,** 21–45.

Bretherton, C. S., and D. S. Battisti, 2000: An interpretation of the results from atmospheric general circulation models forced by the time history of the observed sea surface temperature distribution. *Geophys. Res. Lett.,* **27,** 767–770.

——, C. Smith, and J. M. Wallace, 1992: An intercomparison of methods for finding coupled patterns in climate data. *J. Climate,* **5,** 541–560.

Cayan, D. R., 1992a: Variability of latent and sensible heat fluxes estimated using bulk formulas. *Atmos.–Ocean,* **30,** 1–42.

——, 1992b: Latent and sensible heat-flux anomalies over the northern oceans—The connection to monthly atmospheric circulation. *J. Climate,* **5,** 354–369.

——, 1992c: Latent and sensible heat-flux anomalies over the northern oceans—Driving the sea-surface temperature. *J. Phys. Oceanogr.,* **22,** 859–881.

Cheng, X., G. Nitsche, and J. M. Wallace, 1995: Robustness of low-frequency circulation patterns derived from EOF and rotated EOF analysis. *J. Climate,* **8,** 1709–1713.

Chervin, R. M., and S. H. Schneider, 1976: On determining the statistical significance of climate experiments with general circulation models. *J. Atmos. Sci.,* **33,** 405–412.

Czaja, A., and C. Frankignoul, 1999: Influence of the North Atlantic SST on the atmospheric circulation. *Geophys. Res. Lett.,* **26,** 2969–2972.

——, and J. Marshall, 2000: On the interpretation of AGCMs response to prescribed time-varying SST anomalies. *Geophys. Res. Lett.,* **27,** 1927–1930.

——, and C. Frankignoul, 2002: Observed impact of Atlantic SST anomalies on the North Atlantic Oscillation. *J. Climate,* **15,** 606–623.

Davis, R. E., 1976: Predictability of sea surface temperature and sea level pressure anomalies over the North Pacific Ocean. *J. Phys. Oceanogr.,* **6,** 249–266.

——, 1978: Predictability of sea level pressure anomalies over the North Pacific Ocean. *J. Phys. Oceanogr.,* **8,** 233–246.

Delworth, T. L., 1996: North Atlantic interannual variability in a coupled ocean–atmosphere model. *J. Climate,* **9,** 2356–2375.

Deser, C., and M. L. Blackmon, 1993: Surface climate variations over the North Atlantic Ocean during winter—1900–1989. *J. Climate,* **6,** 1743–1753.

——, and M. S. Timlin, 1997: Atmosphere–ocean interaction on weekly timescales in the North Atlantic and Pacific. *J. Climate,* **10,** 393–408.

Ferranti, L., F. Molteni, and T. N. Palmer, 1994: Impact of localized tropical and extratropical SST anomalies in ensembles of seasonal GCM integrations. *Quart. J. Roy. Meteor. Soc.,* **120,** 1613–1645.

Frankignoul, C., 1985: Sea surface temperature anomalies, planetary waves and air–sea feedback in the middle latitudes. *Rev. Geophys.,* **23,** 357–390.

——, and K. Hasselmann, 1977: Stochastic climate models. 2. Application to sea-surface temperature anomalies and thermocline variability. *Tellus,* **29,** 289–305.

——, and R. W. Reynolds, 1983: Testing a dynamical model for midlatitude sea surface temperature anomalies. *J. Phys. Oceanogr.,* **13,** 1131–1145.

——, A. Czaja, and B. L'Heveder, 1998: Air–sea feedback in the North Atlantic and surface boundary conditions for ocean models. *J. Climate,* **11,** 2310–2324.

Gallimore, R. G., 1995: Simulated ocean–atmosphere interaction in the North Pacific from a GCM coupled to a constant-depth mixed layer. *J. Climate,* **8,** 1721–1737.
Gates, W. L., 1992: AMIP: The Atmospheric Model Intercomparison Project. PCMDI 7, Lawrence Livermore National Laboratory, Livermore, CA, 17 pp.
Gill, A. E., and P. P. Niiler, 1973: The theory of the seasonal variability in the ocean. *Deep-Sea Res.,* **20,** 141–177.
Graham, N. E., T. P. Barnett, and R. Wilde, 1994: On the roles of tropical and midlatitude SSTs in forcing interannual to interdecadal variability in the winter Northern Hemisphere circulation. *J. Climate,* **7,** 1416–1441.
Gu, D. F., and S. G. H. Philander, 1997: Interdecadal climate fluctuations that depend on exchanges between the tropics and extratropics. *Science,* **275,** 805–807.
Hall, N. M. J., J. Derome, and H. Lin, 2001: The extratropical signal generated by a midlatitude SST anomaly. Part I: Sensitivity at equilibrium. *J. Climate,* **14,** 2035–2053.
Haney, R. L., 1985: Midlatitude sea-surface temperature anomalies—A numerical hindcast. *J. Phys. Oceanogr.,* **15,** 787–799.
Harzallah, A., and R. Sadourny, 1995: Internal versus SST-forced atmospheric variability as simulated by an atmospheric general circulation model. *J. Climate,* **8,** 474–495.
Held, I. M., 1983: Stationary and quasi-stationary eddies in the extratropical atmosphere: Theory. *Large Scale Dynamical Processes in the Atmosphere,* R. P. Pearce and B. J. Hoskins, Eds., Academic Press, 127–168.
Hendon, H. H., and D. L. Hartmann, 1982: Stationary waves on a sphere—Sensitivity to thermal feedback. *J. Atmos. Sci.,* **39,** 1906–1920.
Holton, J. R., 1992: *An Introduction to Dynamic Meteorology.* 3d ed. Academic Press, 511 pp.
Hoskins, B. J., and D. J. Karoly, 1981: The steady linear response of a spherical atmosphere to thermal and orographic forcing. *J. Atmos. Sci.,* **38,** 1179–1196.
Junge, M. M., and T. W. N. Haine, 2001: Mechanisms of North Atlantic wintertime sea surface temperature anomalies. *J. Climate,* **14,** 4560–4572.
Kraus, E. B., and J. S. Turner, 1967: A one-dimensional model of the seasonal thermocline, II. *Tellus,* **19,** 98–106.
Kumar, A., and M. P. Hoerling, 1995: Prospects and limitations of seasonal atmospheric GCM predictions. *Bull. Amer. Meteor. Soc.,* **76,** 335–345.
Kushnir, Y., 1994: Interdecadal variations in North Atlantic sea surface temperature and associated atmospheric conditions. *J. Climate,* **7,** 141–157.
——, and N. C. Lau, 1992: The general circulation model response to a North Pacific SST anomaly: Dependence on timescale and pattern polarity. *J. Climate,* **5,** 271–283.
——, and I. M. Held, 1996: Equilibrium atmospheric response to North Atlantic SST anomalies. *J. Climate,* **9,** 1208–1220.
Latif, M., and T. P. Barnett, 1994: Causes of decadal climate variability over the North Pacific and North America. *Science,* **266,** 634–637.
——, and ——, 1996: Decadal climate variability over the North Pacific and North America: Dynamics and predictability. *J. Climate,* **9,** 2407–2423.
Lau, N. C., 1985: Modeling the seasonal dependence of the atmospheric response to observed El Niños in 1962–76. *Mon. Wea. Rev.,* **113,** 1970–1996.
——, and M. J. Nath, 1991: Variability of the baroclinic and barotropic transient eddy forcing associated with monthly changes in the midlatitude storm tracks. *J. Atmos. Sci.,* **48,** 2589–2613.
——, and ——, 1994: A modeling study of the relative roles of tropical and extratropical SST anomalies in the variability of the global atmosphere–ocean system. *J. Climate,* **7,** 1184–1207.
——, and ——, 1996: The role of the ''atmospheric bridge'' in linking tropical Pacific ENSO events to extratropical SST anomalies. *J. Climate,* **9,** 2036–2057.
Luksch, U., and H. von Storch, 1992: Modeling the low-frequency sea surface temperature variability in the North Pacific. *J. Climate,* **5,** 893–906.
Lunkeit, F., and Y. von Detten, 1997: The linearity of the atmospheric response to North Atlantic sea surface temperature anomalies. *J. Climate,* **10,** 3003–3014.
Madden, R. A., 1976: Estimates of the natural variability of time-averaged sea-level pressure. *Mon. Wea. Rev.,* **104,** 942–952.
——, 1983: The effect of the interference of traveling and stationary waves on time variations of the large-scale circulation. *J. Atmos. Sci.,* **40,** 1110–1125.
Manabe, S., and R. J. Stouffer, 1996: Low-frequency variability of surface air temperature in a 1000-year integration of a coupled atmosphere–ocean–land surface model. *J. Climate,* **9,** 376–393.
Marshall, J., H. Johnson, and J. Goodman, 2001: A study of the interaction of the North Atlantic Oscillation with ocean circulation. *J. Climate,* **14,** 1399–1421.
Mehta, V. M., M. J. Suarez, J. V. Manganello, and T. L. Delworth, 2000: Oceanic influence on the North Atlantic Oscillation and associated Northern Hemisphere climate variations: 1959–1993. *Geophys. Res. Lett.,* **27,** 121–124.
Nakamura, H., G. Lin, and T. Yamagata, 1997: Decadal climate variability in the North Pacific during the recent decades. *Bull. Amer. Meteor. Soc.,* **78,** 2215–2225.
Namias, J., 1959: Recent seasonal interaction between North Pacific waters and the overlying atmospheric circulation. *J. Geophys. Res.,* **64,** 631–646.
——, 1965a: Macroscopic association between monthly mean sea-surface temperature and overlying winds. *J. Geophys. Res.,* **70,** 2307–2318.
——, 1965b: Short period climatic fluctuations. *Science,* **147,** 696–706.
——, 1969: Seasonal interactions between the North Pacific Ocean and the atmosphere during the 1960s. *Mon. Wea. Rev.,* **97,** 173–192.
——, 1972: Experiments in objectively predicting some atmospheric and oceanic variables for the winter of 1971–72. *J. Appl. Meteor.,* **11,** 1164–1174.
——, and A. M. Born, 1970: Temporal coherence in North Pacific sea surface temperature patterns. *J. Geophys. Res.,* **75,** 5952–5955.
——, and D. R. Cayan, 1981: Large-scale air–sea interactions and short period climate fluctuations. *Science,* **214,** 869–876.
——, X. Yuan, and D. R. Cayan, 1988: Persistence of North Pacific sea surface temperature and atmospheric flow patterns. *J. Climate,* **1,** 682–703.
Neelin, J. D., D. S. Battisti, A. C. Hirst, F. F. Jin, Y. Wakata, T. Yamagata, and S. E. Zebiak, 1998: ENSO theory. *J. Geophys. Res.,* **103C,** 14 261–14 290.
Niiler, P. P., and E. B. Kraus, 1977: One-dimensional models of the upper ocean. *Modeling and Prediction of the Upper Layers of the Ocean,* E. B. Kraus, Ed., Pergamon, 143–172.
Palmer, T. N., 1995: The influence of north-west Atlantic sea surface temperature: An unplanned experiment. *Weather,* **50,** 413–419.
——, and Z. Sun, 1985: A modeling and observational study of the relationship between sea-surface temperature in the northwest Atlantic and the atmospheric general-circulation. *Quart. J. Roy. Meteor. Soc.,* **111,** 947–975.
Peng, S., and J. S. Whitaker, 1999: Mechanisms determining the atmospheric response to midlatitude SST anomalies. *J. Climate,* **12,** 1393–1408.
——, and W. A. Robinson, 2001: Relationships between atmospheric internal variability and the responses to an extratropical SST anomaly. *J. Climate,* **14,** 2943–2959.
——, A. Mysak, H. Ritchie, J. Derome, and B. Dugas, 1995: The difference between early and middle winter atmospheric response to sea surface temperature anomalies in the northwest Atlantic. *J. Climate,* **8,** 137–157.
——, W. A. Robinson, and M. P. Hoerling, 1997: The modeled atmospheric response to midlatitude SST anomalies and its de-

pendence on background circulation states. *J. Climate,* **10,** 971–987.
——, ——, and S. Li, 2002: North Atlantic SST forcing of the NAO and relationships with intrinsic hemispheric variability. *Geophys. Res. Lett.,* **29** (8), 117 (1–4).
Pitcher, E. J., M. L. Blackmon, G. T. Bates, and S. Munoz, 1988: The effect of North Pacific sea surface temperature anomalies on the January climate of a general circulation model. *J. Atmos. Sci.,* **45,** 172–188.
Ratcliffe, R. A. S., and R. Murray, 1970: New lag associations between North Atlantic sea temperatures and European pressure applied to long-range weather forecasting. *Quart. J. Roy. Meteor. Soc.,* **96,** 226–246.
Roads, J. O., 1989: Linear and nonlinear response to midlatitude surface temperature anomalies. *J. Climate,* **2,** 1014–1040.
Robertson, A. W., C. R. Mechoso, and Y. J. Kim, 2000: The influence of Atlantic sea surface temperature anomalies on the North Atlantic oscillation. *J. Climate,* **13,** 122–138.
Rodwell, M. J., D. P. Rowell, and C. K. Folland, 1999: Oceanic forcing of the wintertime North Atlantic Oscillation and European climate. *Nature,* **398,** 320–323.
Roeckner, E., and Coauthors, 1992: Simulation of the present-day climate with the ECHAM model: Impact of model physics and resolution. MPI Rep. 93, 171 pp. [Available from MPI für Meteorologie, Bundesstr. 55, 20146 Hamburg, Germany.]
——, and Coauthors, 1996: The atmospheric general circulation model ECHAM-4: Model description and simulation of present-day climate. MPI Rep. 218, 90 pp. [Available from MPI für Meteorologie, Bundesstr. 55, 20146 Hamburg, Germany.]
Rowell, D. P., 1998: Assessing potential seasonal predictability with an ensemble of multidecadal GCM simulations. *J. Climate,* **11,** 109–120.
Saravanan, R., 1998: Atmospheric low-frequency variability and its relationship to midlatitude SST variability: Studies using the NCAR Climate System Model. *J. Climate,* **11,** 1386–1404.
——, and J. C. McWilliams, 1998: Advective ocean–atmosphere interaction: An analytical stochastic model with implications for decadal variability. *J. Climate,* **11,** 165–188.
——, G. Danabasoglu, S. C. Doney, and J. C. McWilliams, 2000: Decadal variability and predictability in the midlatitude ocean–atmosphere system. *J. Climate,* **13,** 1073–1097.
Schneider, E. K., and J. L. Kinter, 1994: An examination of internally generated variability in long climate simulations. *Climate Dyn.,* **10,** 181–204.
Seager, R., M. B. Blumenthal, and Y. Kushnir, 1995: An advective atmospheric mixed-layer model for ocean modeling purposes—Global simulation of surface heat fluxes. *J. Climate,* **8,** 1951–1964.
——, Y. Kushnir, M. Visbeck, N. Naik, J. Miller, G. Krahmann, and H. Cullen, 2000: Causes of Atlantic Ocean climate variability between 1958 and 1998. *J. Climate,* **13,** 2845–2862.
——, ——, N. H. Naik, M. A. Cane, and J. Miller, 2001: Wind-driven shifts in the latitude of the Kuroshio–Oyashio extension and generation of SST anomalies on decadal timescales. *J. Climate,* **14,** 4249–4265.
Shukla, J., 1983: Comments on ''natural variability and predictability.'' *Mon. Wea. Rev.,* **111,** 581–585.
Ting, M., 1991: The stationary wave response to a midlatitude SST anomaly in an idealized GCM. *J. Atmos. Sci.,* **48,** 1249–1275.
——, and S. Peng, 1995: Dynamics of early and middle winter atmospheric responses to northwest Atlantic SST anomalies. *J. Climate,* **8,** 2239–2254.
Trenberth, K. E., G. W. Branstator, D. Karoly, A. Kumar, N. C. Lau, and C. Ropelewski, 1998: Progress during TOGA in understanding and modeling global teleconnections associated with tropical sea surface temperatures. *J. Geophys. Res.,* **103C,** 14 291–14 324.
Valdes, P. J., and B. J. Hoskins, 1989: Linear stationary wave simulations of the time-mean climatological flow. *J. Atmos. Sci.,* **46,** 2509–2527.
Venzke, S., M. R. Allen, R. T. Sutton, and D. P. Rowell, 1999: The atmospheric response over the North Atlantic to decadal changes in sea surface temperature. *J. Climate,* **12,** 2562–2584.
von Storch, H., and H. A. Kruse, 1985: The extra-tropical atmospheric response to El Niño events—A multivariate significance analysis. *Tellus,* **37A,** 361–377.
Wallace, J. M., and Q.-R. Jiang, 1987: On the observed structure of interannual variability of the atmosphere/ocean climate system. *Atmospheric and Oceanic Variability,* H. Cattle, Ed., Royal Meteorological Society, 17–43.
Walter, K., U. Luksch, and K. Fraedrich, 2001: A response climatology of idealized midlatitude thermal forcing experiments with and without a storm track. *J. Climate,* **14,** 467–484.
Ward, M. N., and A. Navarra, 1997: Pattern analysis of SST-forced variability in ensemble GCM simulations: Examples over Europe and the tropical Pacific. *J. Climate,* **10,** 2210–2220.
Watanabe, M., and M. Kimoto, 1999: Tropical-extratropical connection in the Atlantic atmosphere–ocean variability. *Geophys. Res. Lett.,* **26,** 2247–2250.
Weare, B. C., 1977: Empirical orthogonal analysis of Atlantic Ocean surface temperature. *Quart. J. Roy. Meteor. Soc.,* **103,** 467–478.
Whitaker, J. S., and P. D. Sardeshmukh, 1998: A linear theory of extratropical synoptic eddy statistics. *J. Atmos. Sci.,* **55,** 237–258.
Zhang, Y., J. M. Wallace, and D. S. Battisti, 1997: ENSO-like decade-to-century scale variability: 1900–93. *J. Climate,* **10,** 1004–1020.
Zwiers, F. W., 1987: Statistical considerations for climate experiments 2. Multivariate tests. *J. Climate Appl. Meteor.,* **26,** 477–487.
——, and V. V. Kharin, 1998: Changes in the extremes of the climate simulated by CCC GCM2 under CO_2 doubling. *J. Climate,* **11,** 2200–2222.
——, X. L. Wang, and J. Sheng, 2000: Effects of specifying bottom boundary conditions in an ensemble of atmospheric GCM simulations. *J. Geophys. Res.,* **105D,** 7295–7315.